

Precision and Accuracy in Quantitative Measurement of Gene Expression from Single-Cell/Nuclei RNA Sequencing Data

3 Ruijia Dai^{1,a}, Ming Zhang^{2,b}, Tianyao Chu^{2,c}, Richard Kopp^{1,d}, Chunling Zhang^{3,e}, Kefu Liu^{2,f},
4 Yue Wang^{4,g}, Xusheng Wang^{5,6,h}, Chao Chen^{2,7,8*,i}, Chunyu Liu^{1,2,3*,j}

5 ¹*Department of Psychiatry, SUNY Upstate Medical University, Syracuse, NY, USA*

6 *²MOE Key Laboratory of Rare Pediatric Diseases & Hunan Key Laboratory of Medical*
7 *Genetics, School of Life Sciences, and Department of Psychiatry, The Second Xiangya Hospital,*
8 *Central South University, Changsha, Hunan, China*

9 *³Department of Neuroscience & Physiology, SUNY Upstate Medical University, Syracuse, NY,*
10 *USA*

11 *⁴Department of Electrical and Computer Engineering, Virginia Polytechnic Institute and State*
12 *University, VA, USA*

13 ⁵Department of Neurology, University of Tennessee Health Science Center, Memphis, TN, USA

14 ⁶*Department of Genetics, Genomics and Informatics, University of Tennessee Health Science
15 Center, Memphis, TN, USA*

16 ⁷*Furong Laboratory, Changsha, Hunan, China*

¹⁷ *⁸Hunan Key Laboratory of Animal Models for Human Diseases, Central South University,*
¹⁸ *Changsha, China*

19

20 Email: liuch@upstate.edu (Liu C), chaochenr@gmail.com (Chen C)

21

22 **Running title:** *Dai R et al / Quantitative Evaluation of Single-Cell Data Quality*

23

24

25

26

27 **Abstract**

28 Single-cell and single-nucleus RNA sequencing (sc/snRNA-Seq) have become essential tools for
29 profiling gene expression across different cell types in biomedical research. While factors like
30 RNA integrity, cell count, and sequencing depth are known to influence data quality, quantitative
31 benchmarks and actionable guidelines are lacking. This gap contributes to variability in study
32 designs and inconsistencies in downstream analyses. In this study, we systematically evaluated
33 quantitative precision and accuracy in expression measures across 23 sc/snRNA-Seq datasets
34 comprising 3,682,576 cells from 339 samples. Precision was assessed using technical replicates
35 based on pseudo-bulks created from subsampling. Accuracy was evaluated using sample-
36 matched scRNA-Seq and pooled-cell RNA-Seq data of mononuclear phagocytes from four
37 species. Our results show that precision and accuracy are generally low at the single-cell level,
38 with reproducibility being strongly influenced by cell count and RNA quality. We establish
39 data-driven thresholds for optimizing study design, recommending at least 500 cells per cell type
40 per individual to achieve reliable quantification. Furthermore, we show that signal-to-noise ratio
41 is a key metric for identifying reproducible differentially expressed genes. To support future
42 research, we developed VICE (Variability In single-Cell gene Expressions), a tool that evaluates
43 sc/snRNA-seq data quality and estimates the true positive rate of differential expression results
44 based on sample size, observed noise levels, and expected effect size. These findings provide
45 practical, evidence-based guidelines to enhance the reliability and reproducibility of sc/snRNA-
46 seq studies.

47 **KEYWORDS:** Single-cell RNA sequencing; Single-nuclei RNA sequencing; Single-cell
48 genomics; Transcriptome; Quality control

49

50

51

52

53

54

55 **Introduction**

56 Single-cell/nuclei RNA sequencing (Sc/snRNA-Seq) is a powerful technology developed for
57 measuring gene expression in individual cells. The first scRNA-Seq study was published in 2009
58 by Tang et al[1]. Smart-seq was developed, enabling the amplification and sequencing of full-
59 length mRNA transcripts from individual cells, characterizing transcriptomes at single-cell
60 resolution. Since then, more technologies have been developed for single-cell profiling[2], with
61 10X chromium and Smart-seq being the two most commonly used methods.

62 Sc/snRNA-Seq has been used in various applications, including identifying novel transcriptional
63 regulatory mechanisms[3], characterizing cell types and tissue compositions[4], studying
64 developmental dynamics and trajectory of different cell types[5, 6], and identifying cell-type-
65 specific changes as biomarkers for disease or treatment responses[7-9]. All these studies rely on
66 accurate and precise measures of gene expression in each cell type. Precision and accuracy in the
67 quantitative measurement of gene expression are defined as the variability of expression across
68 replicates and the degree to which expression measurements match the actual or true values,
69 hereafter referred to as 'precision' and 'accuracy,' respectively. Only when gene expression is
70 quantified precisely and accurately in each sample, can the results of downstream analyses be
71 reproducible and meaningful.

72 Random and systematic technical variability adds noise to the expression measurements in
73 sc/snRNA-Seq[10]. Many zero values are observed in sc/snRNA-Seq data, called 'dropouts'[11].
74 Dropouts can be caused by target genes truly not being expressed, or due to technical factors
75 such as low mRNA input, mRNA degradation, capture efficiency, amplification efficiency, and
76 sequencing depth. These technical factors can reduce precision and cause bias in accuracy of
77 gene expression measurements. Previous studies attempted to assess technical noise in scRNA-
78 Seq data using Spike-ins[12], sample-matched bulk-tissue RNA-Seq data[13], or qPCR[14] as
79 references. However, these methods have rarely been used due to costs and practical limitations.
80 Strategies to improve the quality of single-cell data such as pooling more cells have been
81 developed, but standardized procedures for completing sc/snRNA-Seq are lacking. There is a
82 lack of systematic, quantitative thresholds to guide experimental design, making it challenging to

83 define optimal parameters for achieving reliable results. These factors are often inconsistently
84 evaluated across published studies, resulting in variability in data quality assessment. Practical
85 guidelines—such as the minimum number of cells required per cell type—are either lacking or
86 too vague, leaving researchers without clear direction for ensuring robust data quality in their
87 experiments.

88 We evaluated the precision and accuracy of expression measurements with 23 sc/snRNA-Seq
89 datasets produced on three different platforms published in high-profile journals (Table 1) in the
90 framework as illustrated in **Figure 1**. Initially, we surveyed the cell numbers and missing rates in
91 these sc/snRNA-Seq data, followed by calculating precision in each dataset using technical
92 replicates based on pseudo-bulks. Additionally, we explored the impact of several technical
93 factors, including RNA quality, saturation rate, total reads, and sequencing platform on
94 expression precision. We also evaluated the expression accuracy with four datasets of cultured
95 mononuclear phagocytes from sample-matched pooled-cell RNA-Seq and scRNA-Seq data.
96 Lastly, we evaluated the effect of cell number and other factors on the reproducibility of
97 downstream differential expression (DE) analysis. Based on the evaluation, we provided
98 practical guidelines for future studies. To facilitate future experiment design and data evaluation,
99 we developed a tool we named VICE (Variability In single-Cell gene Expressions)

100 <https://github.com/RujiaDai/VICE>.

101

102 **Results**

103 **Existing sc/snRNA-Seq data have high missing rate**

104 We measured the missing rate for each gene at both the individual-cell and pseudo-bulk levels.
105 Pseudo-bulks were created from single-cell gene expression of a specific cell type within an
106 individual to mimic bulk RNA-Seq data. The missing rate was defined as the proportion of cells
107 with zero expression for a given gene across all individual cells or pseudo-bulks of the same cell
108 type. Individual cells had an average missing rate of 90% (**Figure 2A**), while the pseudo-bulks
109 reduced the average missing rate to 40% (**Figure 2B**). Including more cells in the pseudo-bulks
110 resulted in a lower observed missing rate (Figure S1).

111 Though each project sequenced many cells, we noticed that the number of cells sequenced per

112 cell type per individual was sometimes very small, particularly for minor cell types. Across the
113 14 brain datasets, the average total cell count was 247,190, whereas the average cell number per
114 individual was 34,483 (**Figure 2C**). The number was even much smaller for specific cell types
115 per individual. For instance, the BICCN_HVS study sequenced 353,194 cells and categorized 24
116 cell classes (**Figure 2D**). The largest group of cells in this data comprised an average of 1,021
117 intratelencephalic (IT) neurons from layers 2 and 3, while the smallest group had only an average
118 of 4 somatostatin (SST) chodl inhibitory neurons across the samples, a difference of three orders
119 of magnitude.

120

121 **Low expression precision in sc/snRNA-Seq data**

122 Expression precision was evaluated by the expression variability across technical replicates
123 based on pseudo-bulks in sc/snRNA-Seq data. First, we generated technical replicates based on
124 pseudo-bulks by randomly grouping cells of the same type from the same individual into three
125 groups and totaling expression values of each gene from all cells within each group (Figure S2).
126 We then calculated the coefficient of variation (CV) for each gene to measure the variability of
127 gene expression across the technical replicates based on pseudo-bulks in each cell type. To avoid
128 sampling bias, we calculated the CV 100 times and used the averaged CV to represent the overall
129 precision in the data.

130 Our analysis revealed that the median CV of detected genes across technical replicates based on
131 pseudo-bulks was 0.68 ± 0.24 in the 14 brain datasets (**Figure 3**), which is much higher than the
132 median CV observed in bulk-tissue RNA-Seq[15] (ranging from 0.11 to 0.39) and microarray
133 data[16] (ranging from 0.1 to 0.2). Utilizing cell classification in the BICCN_HVS study, we
134 calculated the CV values at both cell type and subtype levels. The CVs were not significantly
135 different at these two resolution levels, suggesting the observed variability was not driven by
136 heterogeneity in a higher-level cell classification (Figure S3). A similar pattern was noted in
137 independent mouse brain data when different numbers of cells were sequenced, indicating that
138 low precision is a technical challenge in single-cell data across various sample sources (Figure
139 S4).

140 To illustrate the expression variability in multiple tissues, the single-cell RNA-seq data from

141 blood, lung, and lymph nodes were evaluated[17]. A similar CV pattern across cell numbers was
142 observed, consistent with findings in brain tissue data. Regardless of tissue type and cell type,
143 approximately 500 cells are needed to drive CV close to 0.1 (Figure S5).

144 Major cell types exhibited lower CV than minor cell types. For example, excitatory neurons, as
145 the most abundant cell type, had a CV of 0.19 ± 0.20 across datasets. In contrast, the other cell
146 types had a median CV of 0.55 ± 0.40 across datasets, indicating that the precision problem is
147 particularly severe for low-abundance cell types. Additionally, expression CV was negatively
148 correlated with expression abundance (Correlation coefficient = -0.88, p-value < 2.2e-16, Figure
149 S6A). Notably, marker genes have lower CV than other genes (Figure S6B).

150 To compare the expression variability in sc- and snRNA-Seq data, we evaluated three brain
151 microglia samples with both sc- and snRNA-Seq data[18]. We observed almost identical CV
152 patterns in the two data types, indicating that quality issues are a common concern for both
153 (Figure S7). We calculated the percentage of samples achieving a designated precision threshold,
154 a CV of 0.1 or lower for each cell type. There was a striking disparity: the proportion of samples
155 from five distinct datasets that satisfied this precision criterion ranged from 3% to 25%, with an
156 average of 5%, as illustrated in Figure S8A. For example, every sample representing upper-layer
157 IT neurons in the BICCN adult dataset successfully passed the precision assessment (Figure
158 S8B). In the case of the BICCN_HVS dataset, 67% of samples pertaining to IT neurons in layers
159 2 and 3 met the established quality benchmarks (Figure S8C). Conversely, in the other nine
160 datasets, not a single sample reached the requisite levels of precision. This indicates a prevalent
161 problem with gene expression noise in individual samples of these datasets.

162

163 **Expression precision is correlated with number of cells sequenced**

164 We expected that the expression precision would be associated with the number of cells
165 sequenced and aimed to identify the minimum cell number for acceptable precision. To prove the
166 expectation by actual data, we generated technical replicates based on pseudo-bulks with varying
167 numbers of cells, ranging from single cell to the maximum cell number divided by three. The
168 sample with the largest number of total cells in each dataset was utilized for testing. As the
169 number of cells pooled into the technical replicates based on pseudo-bulks increased, the overall

170 variability decreased until it reached a plateau for major cell types (**Figure 4A** and **Figure 4C**).
171 With the small total number of cells sequenced, the minor cell types did not reach a stable CV
172 (Figure S9). Similar correlation coefficients of -0.66 ± 0.07 and -0.78 ± 0.14 were observed
173 between the number of cells in each replicate and median CV in excitatory neuron and
174 oligodendrocyte respectively (p-value < 0.05, **Figure 4B** and **Figure 4D**).

175 The minimum number of cells required for delivering acceptable precision is suggested by data
176 of excitatory neurons. Based on five datasets (BICCN_adult, BICCN_dev, BICCN_trimester1,
177 M1_10X, and BICCN_HVS), approximately 500 cells were required to achieve a median CV
178 close to 0.1 for neurons (**Figure 4A**). None of the other cell types attained CV values as low as
179 0.1 and they all had fewer than 500 cells sequenced.

180

181 **RNA integrity is correlated with expression precision**

182 The cell numbers required for achieving an acceptable precision level in sc/snRNA-Seq data
183 vary across studies, suggesting expression precision may not be solely dependent on the number
184 of cells. We examined the effects of four technical factors, including RNA integrity, sequencing
185 depth, sequencing saturation, and sequencing platform, on expression precision of excitatory
186 neurons.

187 We tested the relationship between RNA integrity, as measured by the RNA integrity number
188 (RIN), and median CV in technical replicates. Two datasets with RIN information available for
189 analysis were used. Samples with higher RIN value tended to have lower CV values (**Figure 5A**
190 and **Figure 5B**). By zooming into replicates with 200 cells, negative correlations were observed
191 between RIN and median CV in the ROSMAP ($R^2 = 0.26$, p-value = 0.06, **Figure 5C**) and
192 autism_PFC ($R^2 = 0.60$, p-value = 0.04, **Figure 5D**) datasets, suggesting that RNA integrity is
193 another factor contributing to expression precision.

194 In the autism_PFC data, we also explored the correlation between median CV and total
195 sequencing depth (p-value = 0.89) and saturation rates (p-value = 0.76), but no significant
196 correlation was found (Figure S10A, Figure S10B). We also compared expression variability
197 across technical replicates in data generated from two different sequencing platforms, 10X
198 Chromium (autsim_PFC) and Smart-seq (MTG). The median CV across detected genes in

199 replicates constructed by 200 cells was used for comparison. No significant difference in gene
200 expression variability was observed between the two technologies (p-value = 0.56, Wilcoxon
201 signed-rank test, Figure S10C), indicating the precision problem is not unique to a specific
202 sequencing platform.

203

204 **Low expression accuracy in scRNA-Seq data associated with the number of cells sequenced**

205 To evaluate the accuracy of gene expression, we compared pooled-cell RNA-Seq data with
206 single-cell RNA-Seq data of cultured mononuclear phagocytes from matched samples (**Figure**
207 **6A**). RNA-seq data from pooled cultured cells (of one type) was referred to as pooled-cell RNA-
208 seq. The gene expressions from pooled-cell RNA-Seq were considered as the ground truth. We
209 used Pearson correlation and linear regression to assess the expression accuracy. In the linear
210 regression model, the ground truth was treated as the independent variable, while the pseudo-
211 bulks from sample-matched scRNA-Seq was the dependent variable. We tested the significance
212 of the slope deviating from one. The significance of the linear regression, combined with the
213 Pearson correlation coefficient, was used to measure expression accuracy. We calculated the
214 expression accuracy independently for each of the four species. To illustrate the relationship
215 between the number of cells and expression accuracy, we performed downsampling experiments,
216 ranging from 1,000 to 1 cell for each sample.

217 The number of genes with good accuracy decreased in down sampling (**Figure 6B**). We
218 observed 3,450 out of 13,907 detected genes with good accuracy as defined by criteria of
219 regression slope of 1 (p-value of 0.05) and correlation coefficient of 0.9 when 1000 cells were
220 analyzed for each sample in mouse data. When each sample contained a single cell, only 100
221 genes showed good accuracy. When data have 500 cells in each sample, the gene accuracy tends
222 to reach a stable value. Similar patterns were observed in data from rat, pig, and rabbit, though
223 pig and rabbit data showed overall worse performance than mouse and rat data (Table S1).

224 The relationship between number of cells and expression accuracy was replicated in the
225 simulation data. In the simulation, scRNA-Seq data of six samples, each with 3000 cells, were
226 synthesized. The pseudo-bulks of 3000 cells in each sample were used as ground truth. We
227 observed that the number of genes with good accuracy increased with larger cell numbers

228 (Figure S11), consistent with results from our real data. Notably, when at least 500 cells were
229 sampled, the number of genes with good accuracy began to stabilize.

230

231 **Noise level and trait effect size interactively affects the reproducibility of differential**
232 **expression analysis in scRNA-Seq data**

233 To assess the impact of data quality on downstream analysis, we conducted a DE analysis in
234 sample-matched scRNA-Seq and pooled-cell RNA-Seq datasets independently, comparing
235 Lipopolysaccharide (LPS)-treated and untreated groups using the edgeR algorithm. Genes were
236 considered significantly differentially expressed (DEGs) when their false discovery rate (FDR)-
237 corrected p-value was less than 0.05. Since we already showed that both expression precision
238 and accuracy were positively correlated with the number of cells sequenced, we employed a
239 down-sampling strategy to investigate the influence of cell number on DE results. By utilizing
240 the DE results in pooled-cell RNA-Seq data as ground truth, we evaluated the overall
241 reproducibility of DE results in scRNA-Seq data with true positive rate, the proportion of actual
242 positive instances that are correctly identified as positive. Notably, as the number of cells
243 increased, the true positive rate improved and had a plateau at about 500 cells (**Figure 7A**). The
244 true positive rates were 0.72, 0.63, 0.62, 0.44 in data from mouse, rat, pig and rabbit, when 500
245 cells were included in each sample.

246 Effect size, which reflects the differences between the compared groups, plays a crucial role in
247 determining the statistical power of a DE analysis. By categorizing the mouse DEGs into three
248 groups based on effect size: high ($|\log_{2}FC| \geq 2$), medium ($1 < |\log_{2}FC| < 2$), and low ($|\log_{2}FC| \leq$
249 1), we observed that DEGs with high and medium effect sizes demonstrate a better true positive
250 rate than those with low effect sizes. DEGs with medium effect sizes still exhibit a relatively
251 lower true positive rate compared to genes with high effect sizes, particularly when the number
252 of cells is limited. (**Figure 7B**).

253 For example, when 500 cells were included in each sample, DEGs with large effect sizes (over
254 two-fold changes) had a true positive rate of 0.73, whereas DEGs with small effect sizes had a
255 true positive rate of only 0.38. When only 50 cells were included in each sample, the true
256 positive rates were 0.41 and 0.09 for DEGs with large and small effect sizes, respectively.

257 This suggested that the relationship between effect size and noise level has an interactive impact
258 on DEG reproducibility. To quantify this combined effect, we adopted signal-to-noise ratio (SNR)
259 metric for each gene, defined as normalized effect size divided by CV. Using mouse data as an
260 example, we found that replicated DEGs exhibited significantly higher SNRs than non-replicated
261 DEGs ($P < 2.2 \times 10^{-12}$, **Figure 7C**). This trend was consistent with the observation that DEGs
262 showing higher expressions tend to have better reproducibility (Figure S12). The factors
263 influencing DEG reproducibility are summarized in **Figure 7D**.

264 To evaluate the applicability of the 500-cell cutoff and the SNR measurement, we applied
265 various cell number cutoffs to an independent dataset from Ruzicka et al.[19], which conducted
266 DE analysis on two schizophrenia postmortem brain cohorts (MCL and Mt Sinai). Using an
267 Exact test, we assessed the reproducibility of DEGs across the two cohorts. At a 500-cell cutoff,
268 cell types with significant DEG reproducibility were clearly distinguishable from those without
269 (Figure S13A). However, reducing the cell-number cutoff to lower thresholds, such as 300 or
270 100 cells—commonly regarded as acceptable in practice—may result in misleading indications
271 of reproducibility. For instance, the Vip neuron emerged as a potential cell type with replicable
272 DEGs at these lower cutoffs, yet its reproducibility was not statistically significant. Moreover,
273 we found that reproduced DEGs exhibited significantly higher SNR ($P = 0.0002$, Figure S13B),
274 effectively distinguishing reproducible genes from non-reproducible ones in this dataset.

275 **Discussion**

276 The use of sc/snRNA-Seq in biological studies has become a common practice, necessitating
277 meticulous evaluation of data quality to avoid misleading or even false findings. The current
278 investigation assesses the expression precision and accuracy of published sc/snRNA-Seq data.
279 By analyzing 23 representative datasets, we demonstrated that the gene expressions per
280 individual measured for most cell types were of low precision and accuracy. We found a robust
281 correlation between the number of cells sequenced and the precision, accuracy, and
282 reproducibility of downstream DE analysis. Only cell types having a large number of cells
283 (minimum 500 cells) sequenced delivered relatively accurate and precise quantification of gene
284 expression and, consequently, credible results of downstream analyses, such as case-control
285 comparisons.

286

287 Many studies have speculated that cell number, RNA integrity, and sequencing depth influence
288 sc/snRNA-seq data quality, but none have systematically quantified these effects across datasets
289 or established actionable thresholds. This lack of clear, reproducible standards has led to
290 inconsistencies in experimental design and, in some cases, unreliable—or even outright
291 incorrect—conclusions. A striking example is Murphy et al.[20], who demonstrated that many of
292 the transcriptional differences reported in Mathys et al.[9] regarding Alzheimer’s disease were
293 false positives, caused by inadequate noise control and flawed differential expression analysis.
294 Alarmingly, this paper —despite its misidentified genes—has been cited over 2,000 times,
295 significantly shaping the Alzheimer’s research landscape. This is just one example; similar issues
296 permeate the field[21-23]. This concern aligns with the findings of previous studies[24, 25]. It is
297 urgent that the single-cell research community recognizes the critical importance of data quality
298 to prevent misleading findings and ensure the reliability of future discoveries. Our study
299 addresses this urgent need by providing a quantitative threshold driven by large datasets, gene-
300 level evaluation metrics, and practical tools and guidance.

301 Our study establishes quantitative thresholds critical for ensuring high-quality single-cell data
302 and results. Prior studies qualitatively recognized that increasing the number of cells improves
303 data quality and reproducibility[26, 27], but the relationship between them is non-linear and the
304 gene expression precision, accuracy and reproducibility saturate at certain cell numbers (Figure
305 4A, Figure 6B, and Figure 7A). Therefore, a quantitative cutoff is required to exclude low-
306 quality genes and samples, similar to standard practices in bulk RNA-seq. This cutoff has never
307 been defined, creating a gap that limits consistency and reliability in single-cell studies. Our
308 systematic evaluation of 23 sc/snRNA-seq datasets of matured cell types from brain and other
309 tissues demonstrates that at least 500 cells per cell type per individual are required for robust
310 measurements—an evidence-based threshold previously missing in the field.

311 The criteria used for evaluating expression precision in this study are standard statistical
312 techniques. We used $CV < 0.1$ as the cutoff for the expression precision in this evaluation. This
313 is based on previous quality evaluations of bulk RNA-Seq data[16]. We believe that holding
314 sc/sn RNA-seq data to the same standard as bulk RNA seq is appropriate and lowering the
315 standard will lead to noisy results and poor reproducibility. Additionally, our evaluation

316 demonstrated that CV tends to stabilize at around 0.1 in single-cell data, as the number of cells
317 increases. However, when constructing the technical replicates based on pseudo-bulks, we
318 assumed homogeneity within one cell type. Such an assumption can be violated by heterogeneity
319 caused by cell subtypes and states, which may explain the minimum CV that is observed.
320 Nonetheless, our results indicated that cell subtype was not the major cause of poor precision in
321 the cell types we evaluated, as the precision at cell type level is not worse than that at subtype
322 level.

323 RNA quality is another crucial factor impacting expression precision. Notably, in the
324 BICCN_HVS study[28], the minimum number of cells required to achieve a CV of 0.1 was 500,
325 but other datasets require even larger numbers of cells. A key factor contributing to this
326 difference may be the use of surgical samples in the BICCN_HVS study, as these samples tend
327 to be less degraded than frozen postmortem brain samples. Ensuring high RNA quality in
328 samples, such as using RNA with RIN values greater than 7, will likely reduce the number of
329 cells required for quality quantification.

330 The signal-to-noise ratio emerges as a pivotal determinant of the reproducibility of DE analysis.
331 Our investigation revealed that DEGs with large effect sizes exhibit superior reproducibility
332 compared to those with smaller effect sizes. When 500 cells were included in each sample where
333 the noise level was low, DEGs with large effect sizes had a true positive rate of 0.73, whereas
334 DEGs with small effect sizes had a true positive rate of only 0.38. When the cell number
335 decreased to 50 cells where the noise level was high, the true positive rates were 0.41 and 0.09
336 for DEGs with large and small effect sizes, respectively. This comparison indicates that the
337 technical noise matters more for the smaller biological effects and technical noise may be
338 manageable for phenotypes associated with pronounced expression changes. Improving data
339 quality becomes more critical in scenarios where the effect size of the phenotype approaches the
340 noise level. This is particularly relevant for many complex diseases, including neuropsychiatric
341 disorders, where the effect size is typically small[29], necessitating an increase in the number of
342 cells to minimize technical noise.

343 This work provides gene-level metrics to help refine reliable signals. Most prior studies assessed
344 data quality at the cell or sample level, which can be biased by highly expressed genes. In
345 contrast, our study introduces a gene-by-gene evaluation framework, enabling precise quality

346 and reproducibility assessments for individual genes—a crucial advancement for downstream
347 analyses like differential expression. Specifically, we introduce the SNR as a key metric for
348 assessing DEG reproducibility, calculated by dividing fold change by CV. Applying this
349 approach to schizophrenia DEGs and mouse data, we found that reproduced DEGs have
350 significantly higher SNR, which effectively distinguishes reproducible genes from non-
351 reproducible ones in this data, providing a practical metric for ensuring reliable single-cell data
352 analysis.

353 We introduce VICE, a powerful tool that enables researchers to assess the quality of existing
354 single-cell data and predict the reliability of differential expression results. With calculated CV
355 values, users can: (1) determine noise levels across different cell types and samples and (2)
356 identify genes with low noise level, ensuring that only high-confidence genes are prioritized for
357 analysis. By inputting cell numbers, effect sizes, and noise levels, VICE estimates the true
358 positive rate for single-cell DE analysis, providing a direct, data-driven framework for
359 optimizing experimental design and result interpretation. For trait-specific analyses, such as DE,
360 VICE can be used to: (1) estimate the true positive rate based on sample size and cell numbers to
361 guide study design; and (2) evaluate DEG reliability by estimating the true positive rate based on
362 signal-to-noise levels rather than relying solely on p-values.

363 We provide the following guidelines for future single-cell research. For general data quality
364 control, we recommend: (1) prioritizing high-quality RNA samples ($\text{RIN} \geq 7$) whenever possible,
365 as degraded RNA increases noise and reduces reproducibility; and (2) ensuring sufficient cell
366 numbers for reliable analysis. We suggest at least 500 cells per individual per cell type for
367 optimal precision. If this is not feasible, focusing on genes with low noise levels is advisable.
368 Adjusting the CV threshold based on trait effect size can help balance precision with dataset
369 constraints. For result reporting, we recommend: (1) routinely reporting CV values and
370 associated power as quality metrics in single-cell data analysis; and (2) providing the median CV
371 for each sample in sc/snRNA-seq experiments to assess sample quality. These benchmarks set
372 optimal standards rather than rigid requirements. Researchers can adapt them as needed, using
373 pseudo-bulk strategies for low cell numbers or adjusting CV thresholds based on effect size. Our
374 approach provides practical, data-driven guidance that supports informed decision-making rather
375 than imposing one-size-fits-all rules.

376 Our findings hold significant implications across multiple domains. Many researchers have
377 reported results from minor cell types in a variety of tissues, but our work casts doubt about the
378 validity of conclusions drawn from much of this research due to insufficient numbers of cells.
379 The accurate identification and comprehensive study of these minor cell types necessitates
380 sequencing more cells. Beyond elucidating the nuances of DE analysis, our results imply low
381 precision and accuracy impacts other analytical methodologies, including cell classification[30],
382 eQTL mapping[31], and the construction of co-expression networks[32]. The effect of cell
383 numbers on other data analyses remains to be explored.

384 Our study rigorously quantifies these effects and provides concrete, data-driven guidelines to
385 improve sc/snRNA-seq studies. Our goal is not to rescue poor experimental designs—there is no
386 simple fix for flawed data. Instead, we define the scale of the problem with precise numbers,
387 highlighting critical pitfalls in single-cell data analysis. We equip researchers with clear,
388 quantitative metrics to assess which genes and samples meet quality standards for reliable
389 downstream analysis. More importantly, we provide practical tools and data-driven cutoffs,
390 ensuring that future studies are designed correctly from the start, minimizing errors and
391 maximizing reproducibility.

392 Conclusion

393 In this study, we conducted a quantitative evaluation of expression precision and accuracy across
394 23 representative sc/snRNA-Seq datasets, revealing significant deficiencies in gene expression
395 measurements—particularly when sequencing a limited number of cells. We demonstrate that the
396 reproducibility of DE analysis is tightly correlated with cell number, emphasizing the need for
397 data-driven thresholds in study design. To improve the reliability and reproducibility of
398 sc/snRNA-Seq studies, we recommend sequencing at least 500 cells per cell type per individual,
399 including minor cell types and RNA quality (RIN \geq 7). Recognizing practical constraints, we
400 provide flexible, evidence-based guidelines rather than rigid requirements. We strongly advocate
401 for quality assessment before downstream analyses to prevent false discoveries. To facilitate this,
402 we developed VICE, a tool that quantifies technical variability, estimates the true positive rate of
403 DE results, and enables data-driven decision-making in sc/snRNA-Seq studies.

404 Materials and methods

405 **Collection of sc/snRNA-Seq data from cortex**

406 A total of 14 brain sc/snRNA-Seq datasets were obtained for analysis. The collected datasets
407 were derived from human brain studies published between 2012 and 2023[8, 9, 28, 34-45].
408 Samples from individuals with brain disorders were excluded from the analysis to prevent
409 biasing the expression profiles. The raw count and cell annotation data were obtained from the
410 original studies. Due to differences in cell classification across studies, we harmonized cell
411 identities into eight major cell types present in the adult brain, namely excitatory neurons,
412 inhibitory neurons, oligodendrocytes, oligodendrocyte precursor cells, astrocytes, microglia,
413 endothelial cells, and pericytes. The annotation of data from BICCN 2023 collection was
414 retained to evaluate cell subtypes. The scRNA-Seq data of blood, lung, and lymph node from
415 Tabula Sapiens Consortium were used for evaluating expression variability in multiple
416 tissues[17].

417 **Collection of sample-matched data from four species**

418 To assess expression accuracy, we utilized four sample-matched scRNA-Seq and pooled-cell
419 RNA-Seq datasets. These datasets were sourced from Hagai et al.[46], encompassing bone
420 marrow-derived mononuclear phagocytes derived from mouse, rat, pig, and rabbit, all subjected
421 to stimulation with either lipopolysaccharide or poly-I:C for a duration of four hours. Within
422 each species, a total of three samples received lipopolysaccharide treatment, while three
423 additional samples were designated as control groups. We employed the preprocessed data
424 provided by Squair et al.[24], which is available at <https://doi.org/10.5281/zenodo.5048449>.

425 **RIN**

426 The RIN is a numerical value that measures the quality of RNA samples. It is calculated before
427 sequencing using an automated analysis of RNA molecules through electrophoresis, such as
428 Agilent 2100 bioanalyzer. The RIN scale ranges from 1 to 10, with 10 indicating fully intact
429 RNA and 1 indicating completely degraded RNA. We obtained the RIN of samples from the
430 original studies.

431 **Processing of sc/snRNA-Seq data**

432 The sc/snRNA-Seq data underwent processing using Seurat version 4[47]. The raw count matrix

433 and cell annotation matrix were used as input to Seurat. We filtered out genes with zero
434 expression in more than 1/1000 of the total cells in each dataset. The proportion of transcripts
435 mapped to mitochondrial genes was calculated for each cell, and cells with 10% or more
436 mitochondrial gene expression were removed to prevent the inclusion of dead cells. Additionally,
437 cells with less than 200 detected genes or those with more than three standard deviations from
438 the mean number of detected genes were excluded. The count data were normalized based on
439 library size and were scaled with a factor of 10,000. The normalized data were then log-
440 transformed.

441 **Marker gene identification**

442 To identify marker genes in the ROSMAP dataset, we utilized a one versus second high strategy
443 at both the cell and pseudo-bulk level. At the cell level, marker genes were identified using
444 Seurat. Genes with a proportion of zero expression greater than 15% in the target cell type were
445 removed prior to marker gene identification. The Wilcoxon signed-rank test was used to assess
446 the expression difference, and genes with a log2FC greater than 1 and FDR-corrected p-value
447 less than 0.05 were defined as marker genes. At the pseudo-bulk level, pseudo-bulks were
448 constructed by aggregating gene expression for the same cell type from the same individual.
449 Marker genes were then tested using DESeq2[48], and the likelihood ratio test was utilized to
450 evaluate the expression difference between the two cell groups. Marker genes with a log2FC
451 greater than 2 and FDR-corrected p-value less than 0.05 were defined as marker genes at the
452 pseudo-bulk level. Finally, marker genes supported by both cell- and pseudo-bulk-level tests
453 were selected as final marker genes.

454 **Technical replicate construction and CV calculation**

455 To generate technical replicates based on pseudo-bulks for each cell type, cells in the count
456 matrix were randomly divided into three groups for the same individual. The count expression
457 for each gene was then summed within each group. The CV value was calculated for each gene
458 using the following formula:

$$\text{Formula 1: } CVi = \frac{sd(x)}{mean(x)}$$

459 , where x represents the gene expression of gene i across three replicates of a specific cell type.

460 To ensure the robustness of technical replicates, the cell groupings and CV calculations were
461 repeated 100 times, and the average CV across 100 samplings was used.

462 **CV-cell-number relationship in data with cell class and subclass annotations**

463 To compare the relationship between CV values and the number of sequenced cells in the mouse
464 class and subclass data, a Student's t-test was used (Figure S3). To compare the relationship
465 between CV values and the number of sequenced cells in the mouse class and subclass data when
466 different number of cells were sequenced, we used a two-sample Z-test (Figure S4). The null
467 hypothesis was that the slope in the regression model testing the relationship between the number
468 of cells and CV values was the same in the class and subclass data. We calculated the difference
469 in slope between the two datasets using the following formula:

470 *Formula 2:*
$$diff = \frac{b_1 - b_2}{\sqrt{se_1^2 + se_2^2}}$$

471 , where b1 and b2 were the coefficients, and se1 and se2 were the standard errors from the
472 regression model in the class and subclass data, respectively. We then used the area of the
473 standard normal curve corresponding to the calculated difference to determine the probability in
474 a two-tailed manner.

475 **Data simulation**

476 Single-cell count data was simulated based on a negative binomial model using the R package
477 Splatter[49]. Two conditions were generated with the “group” simulation, with between 10 and
478 3000 cells per sample and three replicates per condition. The proportion of differentially
479 expressed genes (‘de.prob’) was set to 0.25.

480 **Evaluation of expression accuracy**

481 Since no single statistic is sufficient to describe accuracy, we developed a composite criterion
482 that captures the bias and distance from ground truth simultaneously using Pearson correlation
483 and a linear regression model. The scRNA-Seq data were summarized by pseudo-bulks first. The
484 pseudo-bulks were normalized by the library size and were transformed into log2-transformed
485 counts per million (CPM). Then the batch effect between pseudo-bulks and pooled-cell RNA-
486 Seq data was corrected using the combat function in the sva package[50]. Pearson correlation
487 between sample-matched scRNA-Seq and pooled-cell RNA-Seq was calculated for each gene. In

488 the linear regression model, the expression in pooled-cell RNA-Seq was treated as the
489 independent variable and expression in scRNA-Seq was treated as the dependent variable. The
490 intercept of linear regression model was set to 0. By setting offset in function lm in R, the
491 significance of slope deviating from 1 was tested. Good accuracy was defined as correlation
492 coefficient over 0.9 and p-value of linear regression over 0.05.

493 **DE analysis**

494 DE analysis was carried out on both scRNA-Seq and pooled-cell RNA-Seq datasets to examine
495 the expression disparities between samples treated with lipopolysaccharide and the control
496 samples. For scRNA-Seq data, DE analysis was performed on pseudo-bulk data using the
497 likelihood ratio test approach provided by edgeR[51]. For pooled-cell RNA-Seq data, edgeR was
498 performed on the count data directly. Genes exhibiting an FDR corrected p-value of less than
499 0.05 were classified as DEGs. We assessed the consistency between DE results obtained from
500 single-cell and pooled-cell RNA-Seq with true positive rate which denotes the proportion of
501 DEGs identified in pooled-cell RNA-Seq that were also replicated in the scRNA-Seq data.

502 **Application of DE analysis to Ruzicka et al.**

503 The schizophrenia DE results were obtained from the supplementary materials of Ruzicka et al.
504 This study includes samples from the Mt Sinai and MCL cohorts. DEGs were defined as genes
505 with $\log_2 \text{FC} > 0.1$ and $\text{FDR} < 0.05$. Replicated DEGs were those that met the DE criteria in
506 both cohorts. The Exact test[52] was performed to assess the statistical significance of DEG
507 replication.

508

509 **Data and code availability**

510 The data supporting the findings of this study are publicly available, with details for accessing
511 the datasets provided in **Table 1**. The code for this paper can be found at
512 <https://github.com/RujiaDai/VICE> and <https://ngdc.cncb.ac.cn/biocode/tool/BT7673>.

513

514 **Declaration of AI and AI-assisted technologies**

515 During the preparation of this work the authors used ChatGPT to improve the clarity, grammar,
516 and readability of the text. After using this tool/service, the authors reviewed and edited the
517 content as needed and take full responsibility for the content of the publication.

518

519 **CRediT author statement**

520 Rujia Dai, Chunyu Liu, and Chao Chen contributed to conceptualization. Rujia Dai, Tianyao Chu,
521 Ming Zhang contributed to formal analysis, data curation, validation, software and methodology.
522 Rujia Dai and Chunyu Liu contributed to the writing of the original draft. Chunling Zhang,
523 Richard Kopp, Kefu Liu, Xusheng Wang, Yue Wang contributed to the investigation, review and
524 editing. Chunyu Liu, and Chao Chen contributed to funding acquisition, supervision, and project
525 administration.

526

527 **Competing interests**

528 The authors declare no competing interests.

529

530 **Acknowledgment**

531 We thank all the participants in studies for making the data available. We also thank Sidney
532 Wang for invaluable guidance and expertise in the experimental design and data analysis. This
533 work was supported by NIH grants U01MH122591, U01MH116489, R01MH110920,
534 U01MH103340, and R01MH126459; the National Natural Science Foundation of China
535 82022024 and 31970572; the science and technology innovation Program of Hunan Province
536 2021RC4018 and 2021RC5027. This work was supported in part by the Bioinformatics Center,
537 Xiangya Hospital, and Central South University.

538

539 **References**

540 [1] Tang F, Barbacioru C, Wang Y, Nordman E, Lee C, Xu N, et al. mRNA-Seq whole-transcriptome
541 analysis of a single cell. Nat Methods 2009;6:377-82.

542 [2] Svensson V, Vento-Tormo R, Teichmann SA. Exponential scaling of single-cell RNA-seq in the past
543 decade. *Nat Protoc* 2018;13:599-604.

544 [3] Cuomo ASE, Nathan A, Raychaudhuri S, MacArthur DG, Powell JE. Single-cell genomics meets
545 human genetics. *Nat Rev Genet* 2023;24:535-49.

546 [4] Network BICC. A multimodal cell census and atlas of the mammalian primary motor cortex. *Nature*
547 2021;598:86-102.

548 [5] Eze UC, Bhaduri A, Haeussler M, Nowakowski TJ, Kriegstein AR. Single-cell atlas of early human
549 brain development highlights heterogeneity of human neuroepithelial cells and early radial glia. *Nat*
550 *Neurosci* 2021;24:584-94.

551 [6] Nowakowski TJ, Bhaduri A, Pollen AA, Alvarado B, Mostajo-Radji MA, Di Lullo E, et al.
552 Spatiotemporal gene expression trajectories reveal developmental hierarchies of the human cortex.
553 *Science* 2017;358:1318-23.

554 [7] Ruzicka WB, Mohammadi S, Fullard JF, Davila-Velderrain J, Subburaju S, Tso DR, et al. Single-cell
555 multi-cohort dissection of the schizophrenia transcriptome. *medRxiv* 2022;2022.08.31.22279406.

556 [8] Velmeshev D, Schirmer L, Jung D, Haeussler M, Perez Y, Mayer S, et al. Single-cell genomics
557 identifies cell type-specific molecular changes in autism. *Science* 2019;364:685-9.

558 [9] Mathys H, Davila-Velderrain J, Peng Z, Gao F, Mohammadi S, Young JZ, et al. Single-cell
559 transcriptomic analysis of Alzheimer's disease. *Nature* 2019;570:332-7.

560 [10] Bacher R, Kendziora C. Design and computational analysis of single-cell RNA-sequencing
561 experiments. *Genome Biol* 2016;17:63.

562 [11] Lahnemann D, Koster J, Szczurek E, McCarthy DJ, Hicks SC, Robinson MD, et al. Eleven grand
563 challenges in single-cell data science. *Genome Biol* 2020;21:31.

564 [12] Brennecke P, Anders S, Kim JK, Kolodziejczyk AA, Zhang X, Proserpio V, et al. Accounting for
565 technical noise in single-cell RNA-seq experiments. *Nat Methods* 2013;10:1093-5.

566 [13] Hicks SC, Townes FW, Teng M, Irizarry RA. Missing data and technical variability in single-cell
567 RNA-sequencing experiments. *Biostatistics* 2018;19:562-78.

568 [14] Wu AR, Neff NF, Kalisky T, Dalerba P, Treutlein B, Rothenberg ME, et al. Quantitative assessment
569 of single-cell RNA-sequencing methods. *Nat Methods* 2014;11:41-6.

570 [15] Li S, Tighe SW, Nicolet CM, Grove D, Levy S, Farmerie W, et al. Multi-platform assessment of
571 transcriptome profiling using RNA-seq in the ABRF next-generation sequencing study. *Nat Biotechnol*
572 2014;32:915-25.

573 [16] Consortium M, Shi L, Reid LH, Jones WD, Shippy R, Warrington JA, et al. The MicroArray Quality
574 Control (MAQC) project shows inter- and intraplatform reproducibility of gene expression measurements.
575 *Nat Biotechnol* 2006;24:1151-61.

576 [17] Tabula Sapiens C, Jones RC, Karkanias J, Krasnow MA, Pisco AO, Quake SR, et al. The Tabula
577 Sapiens: A multiple-organ, single-cell transcriptomic atlas of humans. *Science* 2022;376:eabl4896.

578 [18] Thrupp N, Sala Frigerio C, Wolfs L, Skene NG, Fattorelli N, Poovathingal S, et al. Single-Nucleus
579 RNA-Seq Is Not Suitable for Detection of Microglial Activation Genes in Humans. *Cell Rep*
580 2020;32:108189.

581 [19] Ruzicka WB, Mohammadi S, Fullard JF, Davila-Velderrain J, Subburaju S, Tso DR, et al. Single-
582 cell multi-cohort dissection of the schizophrenia transcriptome. *Science* 2024;384:eadg5136.

583 [20] Murphy AE, Fancy N, Skene N. Avoiding false discoveries in single-cell RNA-seq by revisiting the
584 first Alzheimer's disease dataset. *Elife* 2023;12.

585 [21] Lau SF, Cao H, Fu AKY, Ip NY. Single-nucleus transcriptome analysis reveals dysregulation of
586 angiogenic endothelial cells and neuroprotective glia in Alzheimer's disease. *Proc Natl Acad Sci U S A*
587 2020;117:25800-9.

588 [22] Soreq L, Bird H, Mohamed W, Hardy J. Single-cell RNA sequencing analysis of human Alzheimer's
589 disease brain samples reveals neuronal and glial specific cells differential expression. *PLoS One*
590 2023;18:e0277630.

591 [23] Liu CS, Park C, Ngo T, Saikumar J, Palmer CR, Shahnaee A, et al. RNA Isoform Diversity in
592 Human Neurodegenerative Diseases. *eNeuro* 2024;11.

593 [24] Squair JW, Gautier M, Kathe C, Anderson MA, James ND, Hutson TH, et al. Confronting false
594 discoveries in single-cell differential expression. *Nat Commun* 2021;12:5692.

595 [25] Soneson C, Robinson MD. Bias, robustness and scalability in single-cell differential expression
596 analysis. *Nat Methods* 2018;15:255-61.

597 [26] Polioudakis D, de la Torre-Ubieta L, Langerman J, Elkins AG, Shi X, Stein JL, et al. A Single-Cell
598 Transcriptomic Atlas of Human Neocortical Development during Mid-gestation. *Neuron* 2019;103:785-
599 801 e8.

600 [27] Lahnemann D, Koster J, Szczurek E, McCarthy DJ, Hicks SC, Robinson MD, et al. Eleven grand
601 challenges in single-cell data science. *Genome Biol* 2020;21:31.

602 [28] Johansen N, Somasundaram S, Travaglini KJ, Yanny AM, Shumyatcher M, Casper T, et al.
603 Interindividual variation in human cortical cell type abundance and expression. *Science*
604 2023;382:eadf2359.

605 [29] Gandal MJ, Zhang P, Hadjimichael E, Walker RL, Chen C, Liu S, et al. Transcriptome-wide
606 isoform-level dysregulation in ASD, schizophrenia, and bipolar disorder. *Science* 2018;362.

607 [30] Saliba AE, Westermann AJ, Gorski SA, Vogel J. Single-cell RNA-seq: advances and future
608 challenges. *Nucleic Acids Res* 2014;42:8845-60.

609 [31] van der Wijst M, de Vries DH, Groot HE, Trynka G, Hon CC, Bonder MJ, et al. The single-cell
610 eQTLGen consortium. *Elife* 2020;9.

611 [32] Su C, Xu Z, Shan X, Cai B, Zhao H, Zhang J. Cell-type-specific co-expression inference from single
612 cell RNA-sequencing data. *Nat Commun* 2023;14:4846.

613 [33] Darmanis S, Sloan SA, Zhang Y, Enge M, Caneda C, Shuer LM, et al. A survey of human brain
614 transcriptome diversity at the single cell level. *Proc Natl Acad Sci U S A* 2015;112:7285-90.

615 [34] Lake BB, Chen S, Sos BC, Fan J, Kaeser GE, Yung YC, et al. Integrative single-cell analysis of
616 transcriptional and epigenetic states in the human adult brain. *Nat Biotechnol* 2018;36:70-80.

617 [35] Nagy C, Maitra M, Tanti A, Suderman M, Theroux JF, Davoli MA, et al. Single-nucleus
618 transcriptomics of the prefrontal cortex in major depressive disorder implicates oligodendrocyte precursor
619 cells and excitatory neurons. *Nat Neurosci* 2020;23:771-81.

620 [36] Hodge RD, Bakken TE, Miller JA, Smith KA, Barkan ER, Graybuck LT, et al. Conserved cell types
621 with divergent features in human versus mouse cortex. *Nature* 2019;573:61-8.

622 [37] Bakken TE, Jorstad NL, Hu Q, Lake BB, Tian W, Kalmbach BE, et al. Comparative cellular analysis
623 of motor cortex in human, marmoset and mouse. *Nature* 2021;598:111-9.

624 [38] Li M, Santpere G, Imamura Kawasawa Y, Evgrafov OV, Gulden FO, Pochareddy S, et al. Integrative
625 functional genomic analysis of human brain development and neuropsychiatric risks. *Science* 2018;362.

626 [39] Agarwal D, Sandor C, Volpato V, Caffrey TM, Monzon-Sandoval J, Bowden R, et al. A single-cell
627 atlas of the human substantia nigra reveals cell-specific pathways associated with neurological disorders.
628 *Nat Commun* 2020;11:4183.

629 [40] Zhou Y, Song WM, Andhey PS, Swain A, Levy T, Miller KR, et al. Human and mouse single-
630 nucleus transcriptomics reveal TREM2-dependent and TREM2-independent cellular responses in
631 Alzheimer's disease. *Nat Med* 2020;26:131-42.

632 [41] Morabito S, Miyoshi E, Michael N, Shahin S, Martini AC, Head E, et al. Single-nucleus chromatin
633 accessibility and transcriptomic characterization of Alzheimer's disease. *Nat Genet* 2021;53:1143-55.

634 [42] Yao Z, van Velthoven CTJ, Nguyen TN, Goldy J, Sedeno-Cortes AE, Baftizadeh F, et al. A
635 taxonomy of transcriptomic cell types across the isocortex and hippocampal formation. *Cell*
636 2021;184:3222-41 e26.

637 [43] Velmeshev D, Perez Y, Yan Z, Valencia JE, Castaneda-Castellanos DR, Wang L, et al. Single-cell
638 analysis of prenatal and postnatal human cortical development. *Science* 2023;382:eadf0834.

639 [44] Braun E, Danan-Gotthold M, Borm LE, Lee KW, Vinsland E, Lonnerberg P, et al. Comprehensive
640 cell atlas of the first-trimester developing human brain. *Science* 2023;382:eadf1226.

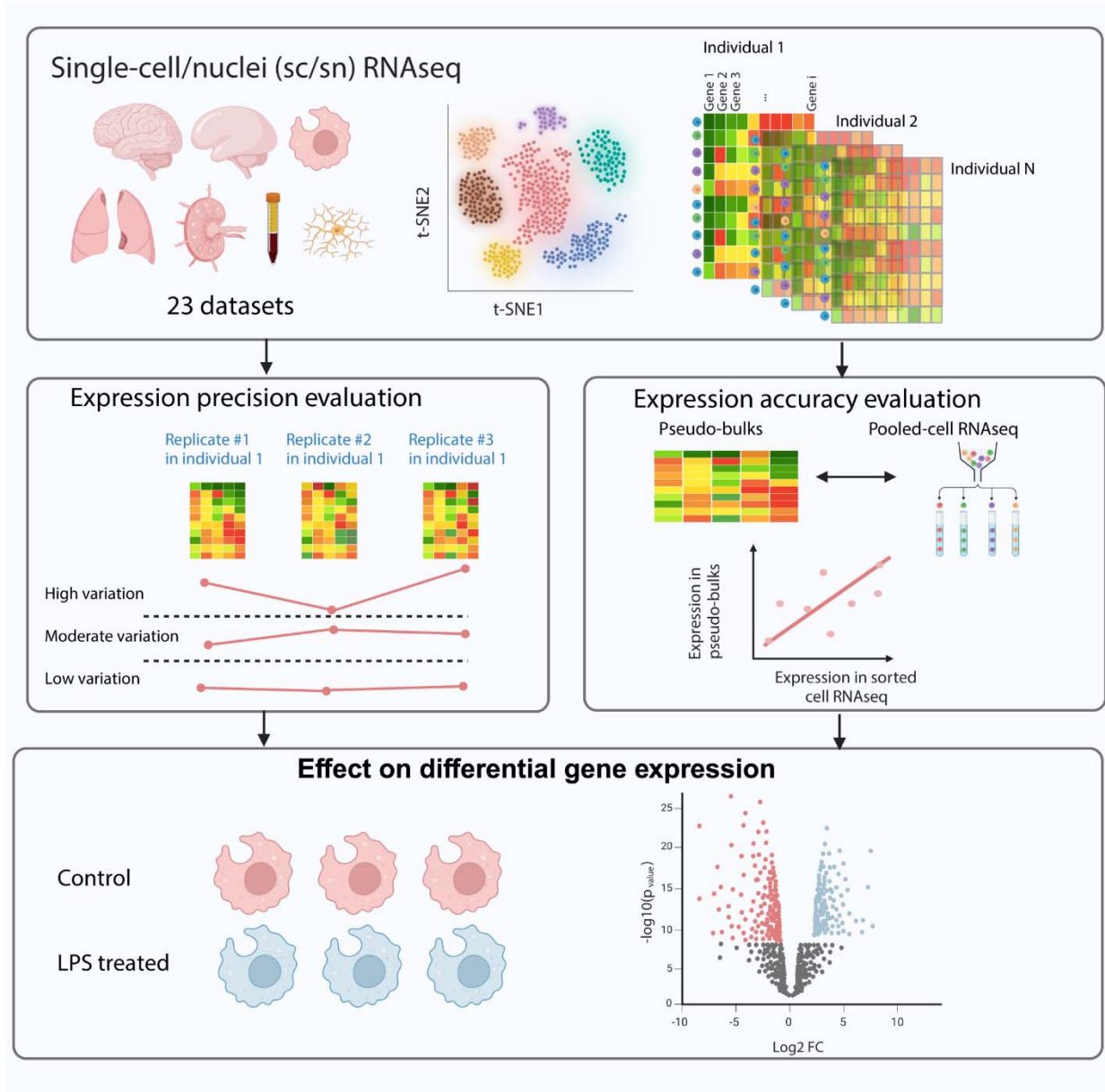
641 [45] Siletti K, Hodge R, Mossi Albiach A, Lee KW, Ding SL, Hu L, et al. Transcriptomic diversity of cell
642 types across the adult human brain. *Science* 2023;382:eadd7046.

643 [46] Hagai T, Chen X, Miragaia RJ, Rostom R, Gomes T, Kunowska N, et al. Gene expression variability
644 across cells and species shapes innate immunity. *Nature* 2018;563:197-202.
645 [47] Hao Y, Hao S, Andersen-Nissen E, Mauck WM, 3rd, Zheng S, Butler A, et al. Integrated analysis of
646 multimodal single-cell data. *Cell* 2021;184:3573-87 e29.
647 [48] Love MI, Huber W, Anders S. Moderated estimation of fold change and dispersion for RNA-seq data
648 with DESeq2. *Genome Biol* 2014;15:550.
649 [49] Zappia L, Phipson B, Oshlack A. Splatter: simulation of single-cell RNA sequencing data. *Genome*
650 *Biol* 2017;18:174.
651 [50] Leek JT, Johnson WE, Parker HS, Jaffe AE, Storey JD. The sva package for removing batch effects
652 and other unwanted variation in high-throughput experiments. *Bioinformatics* 2012;28:882-3.
653 [51] Robinson MD, McCarthy DJ, Smyth GK. edgeR: a Bioconductor package for differential expression
654 analysis of digital gene expression data. *Bioinformatics* 2010;26:139-40.
655 [52] Wang M, Zhao Y, Zhang B. Efficient Test and Visualization of Multi-Set Intersections. *Sci Rep*
656 2015;5:16923.

657

658

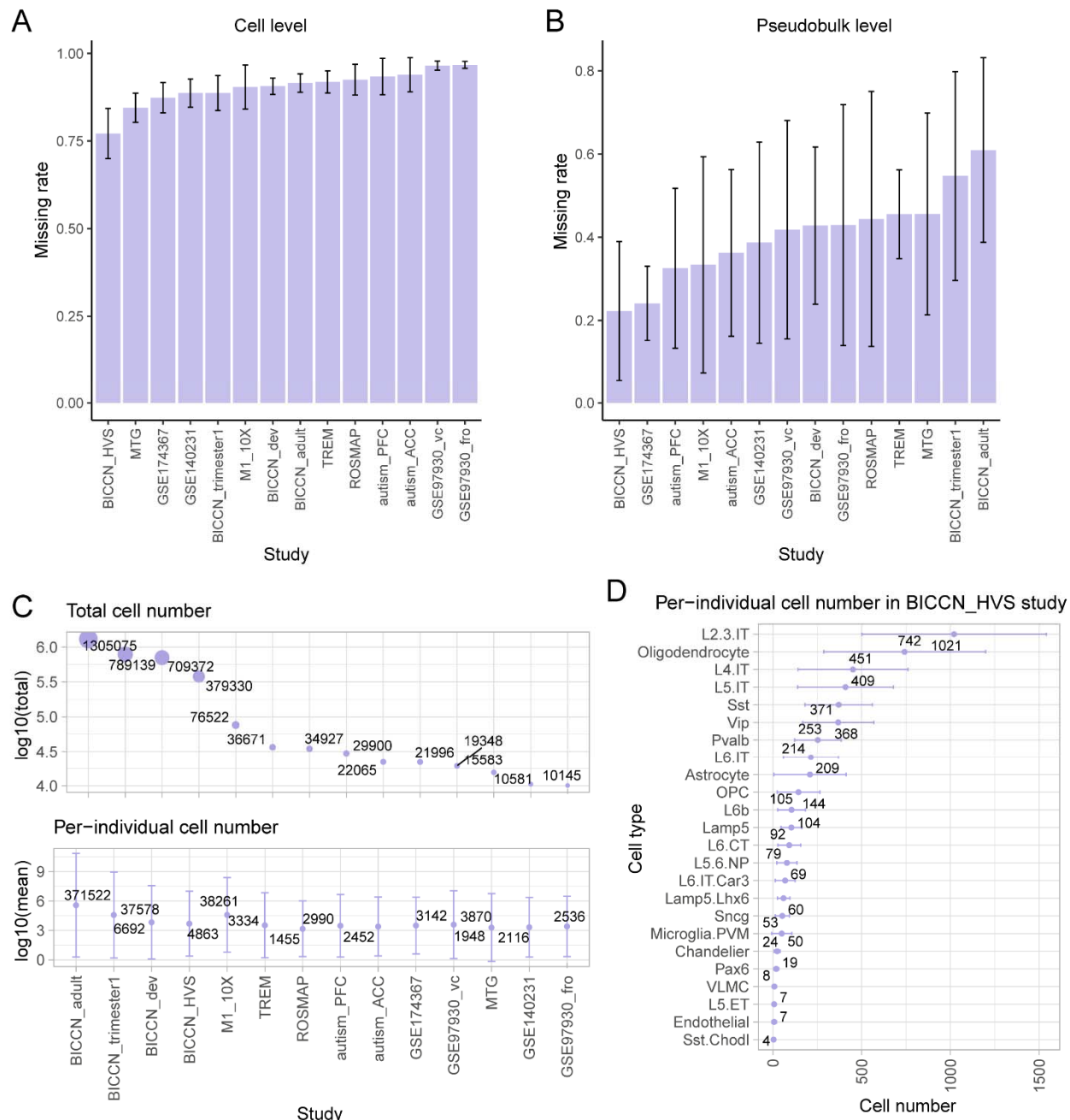
659 **Figures**



660

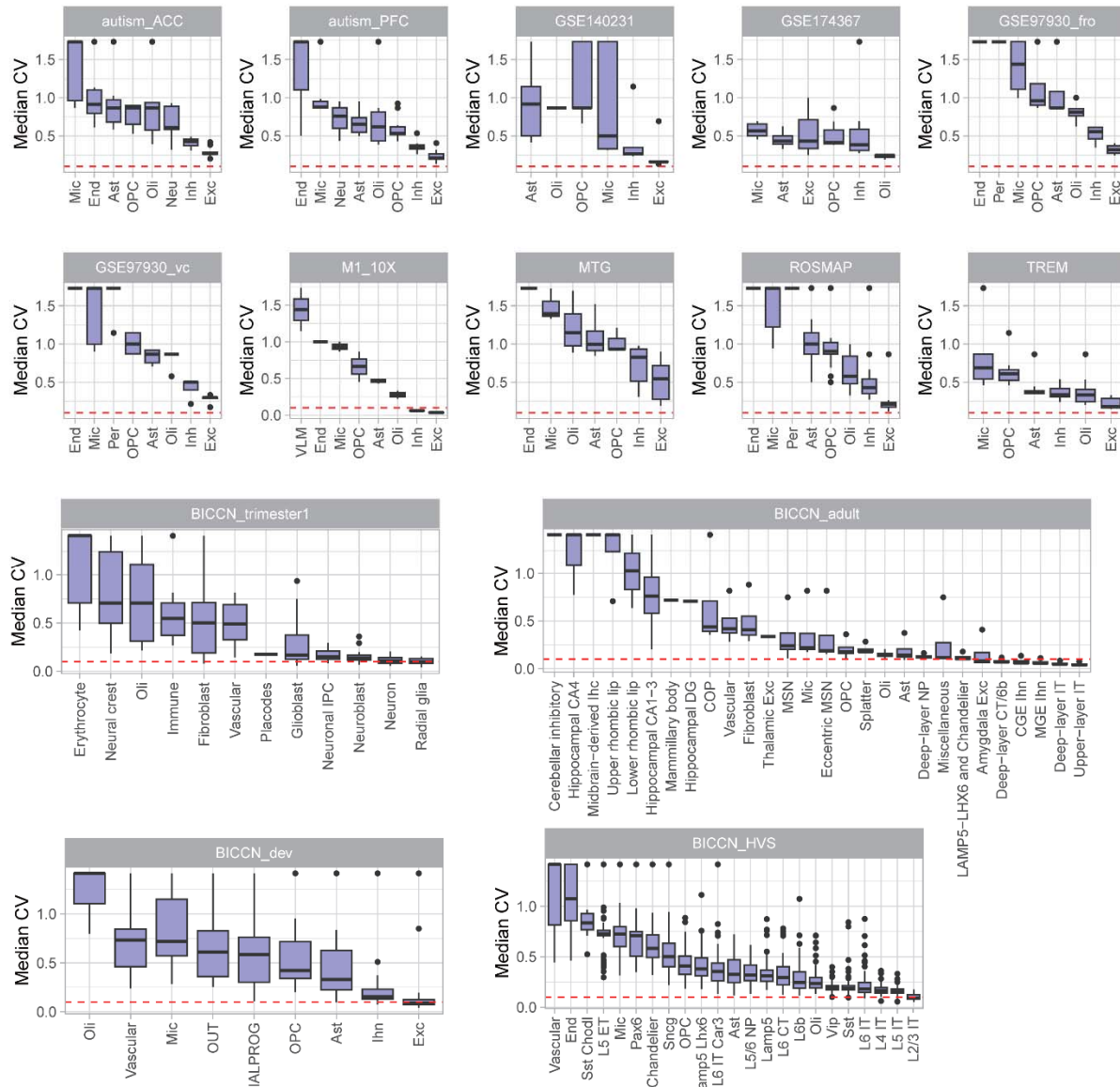
661 **Figure 1 Overview of the study.** Framework for evaluating the expression precision and
662 accuracy of sc/snRNA-Seq across datasets and platforms. We assessed the precision and
663 accuracy of gene expression measurements using 23 sc/snRNA-Seq datasets generated on three
664 platforms. These datasets, published in high-profile journals, were derived from large consortium
665 efforts, including the BICCN, reflecting current technological standards. Our analysis began with
666 a survey of cell numbers and missing rates across datasets, followed by the evaluation of
667 precision based on technical replicates. We then examined the influence of technical factors such
668 as RNA quality, sequencing saturation rate, total read counts, and platform type on expression

669 precision. To assess accuracy, we compared scRNA-Seq data from four cultured mononuclear
 670 phagocyte datasets with corresponding pooled-cell RNA-Seq data from the same samples.
 671 Finally, we analyzed the effects of cell numbers and other factors on the reproducibility of
 672 downstream differential expression analyses. This figure was created with BioRender.com.
 673 Sc/snRNA-Seq, Single-cell/nuclei RNA sequencing expression measures; BICCN, BRAIN
 674 Initiative Cell Census Network.



675

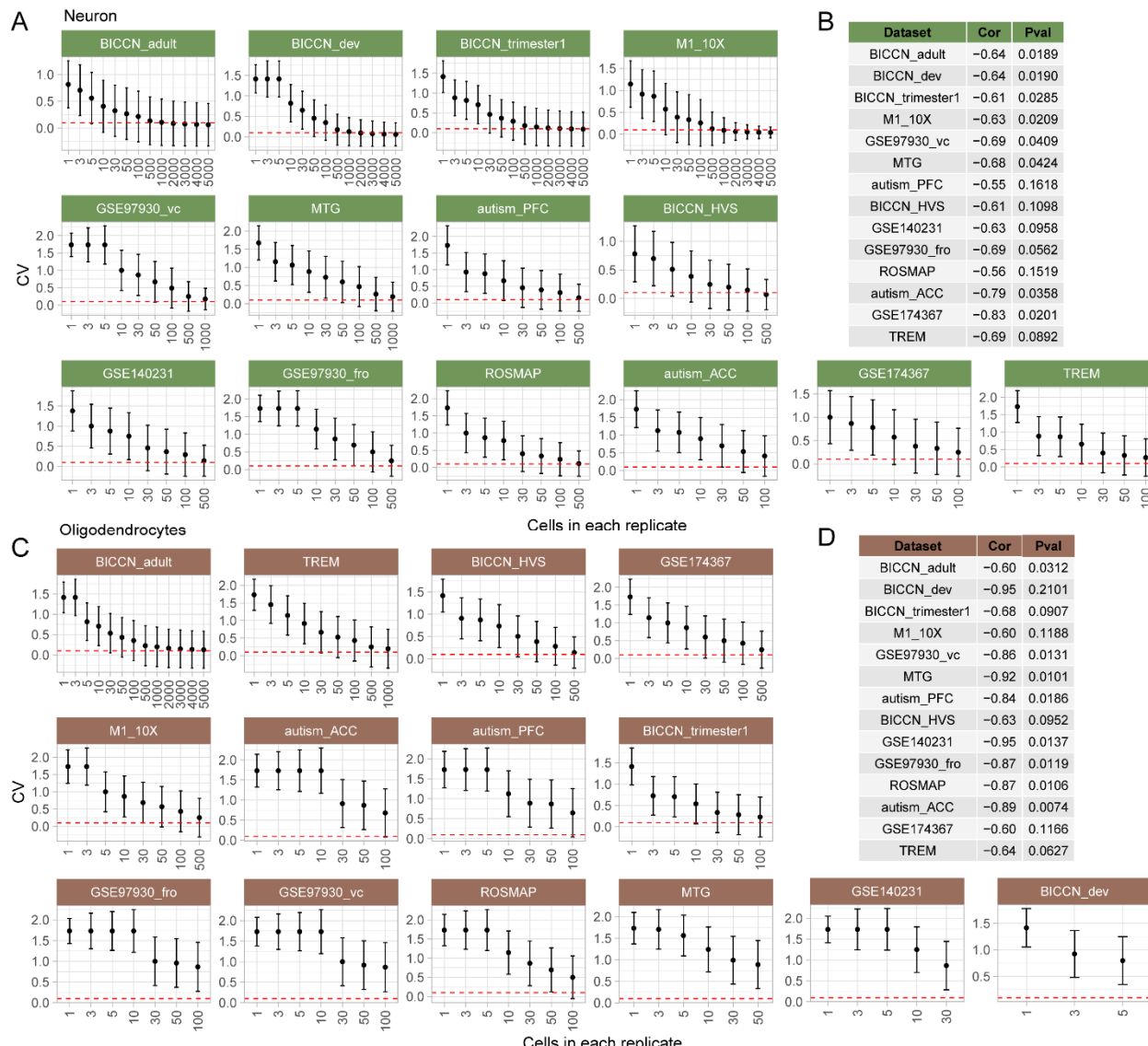
676 **Figure 2 Missing rates and cell numbers in the 14 datasets.** **A.** Missing rate per gene at
 677 individual cell level. **B.** Missing rate per gene at the pseudo-bulk level. **C.** Total number of cells
 678 studied, along with the average number of cells per individual. The cell count per individual was
 679 calculated by dividing the total number of cells by the number of individuals in the study. Cell
 680 numbers were log10-transformed for better visualization. **D.** An illustrative example showcasing
 681 the average number of cells per individual, specifically drawn from the BICCN_HVS study.



682

683 **Figure 3 Gene expression precision evaluated by technical replicates in sc/snRNA-Seq data.**
 684 We calculated gene expression variability as the CV of gene expression in three technical

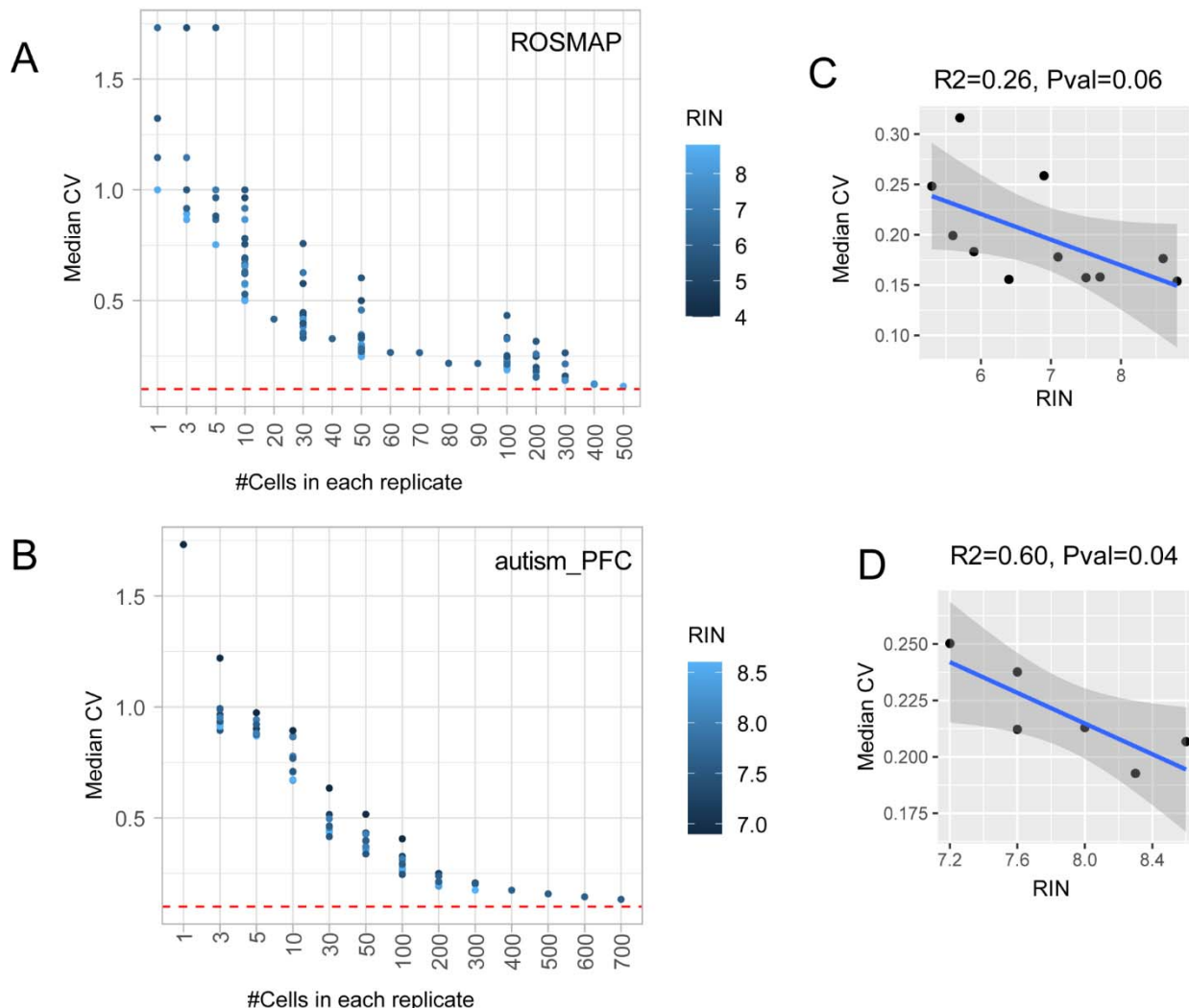
685 replicates based on pseudo-bulks for each gene. The sample with the largest number of total cells
 686 in each dataset was used for illustration. The red dashed line denotes the CV thresholds of 0.1,
 687 which is a threshold recommended for bulk-tissue gene expression quality control processing[16].
 688 CV, coefficient of variation.



689

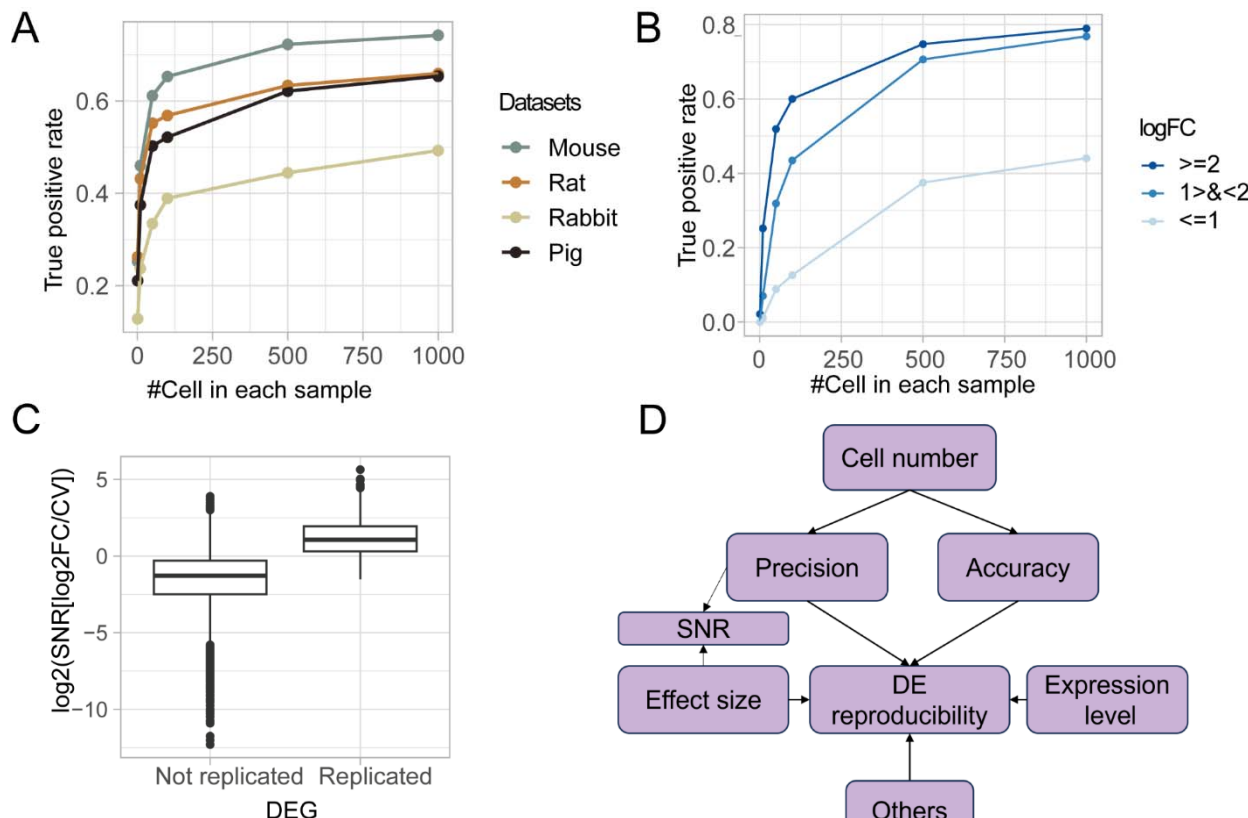
690 **Figure 4 Relationship between cell number and gene expression precision.** **A.** CV values in
 691 down-sampled neurons. **B.** Pearson correlation coefficient and p value between neuron cell
 692 numbers in replicate and median CV. **C.** CV values in down-sampled oligodendrocytes. **D.**
 693 Pearson correlation coefficient and p-value between oligodendrocyte cell numbers in replicate
 694 and median CV. To enhance visual clarity, the number of cells in each replicate was capped at

695 5000. The Red dashed line denotes a CV of 0.1. Cor, Pearson correlation coefficient; Pval, p-
696 value.



697

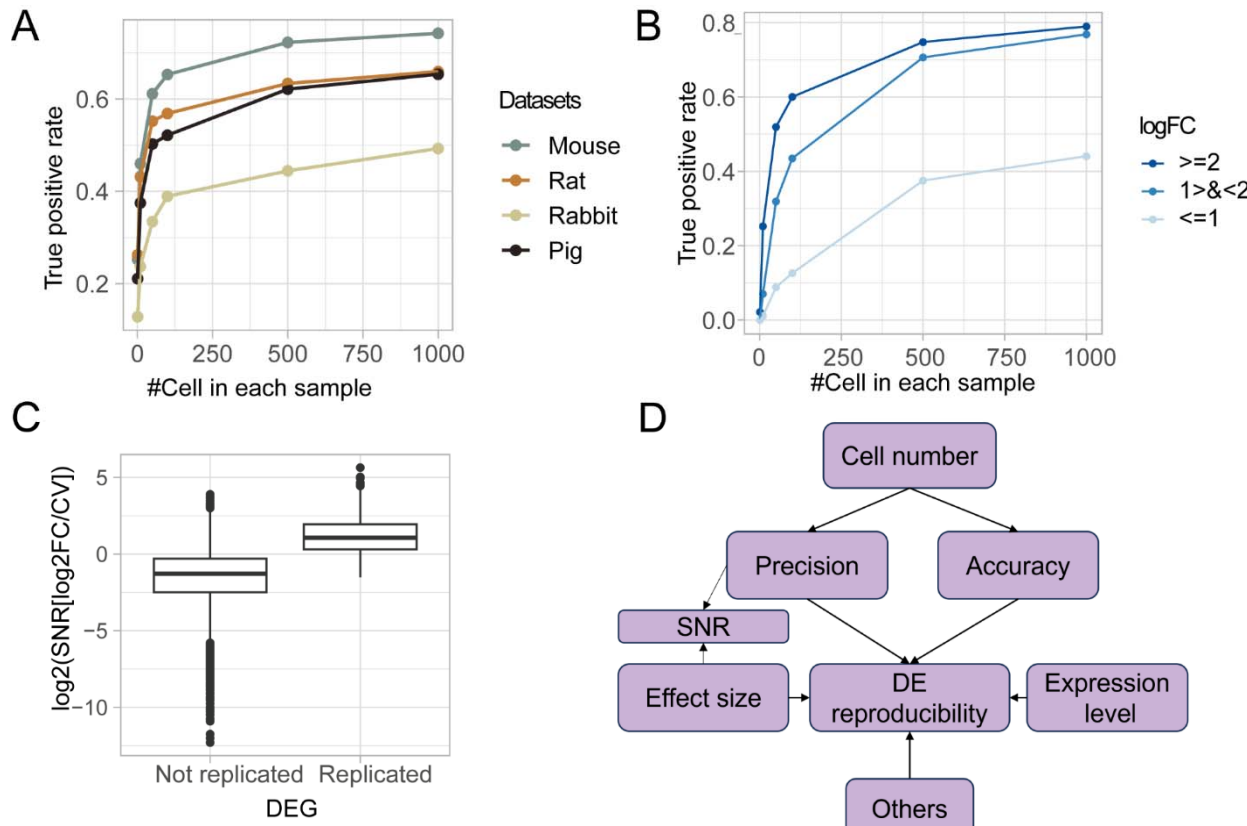
698 **Figure 5 Association between RNA integrity and gene expression variability across**
699 **technical replicates in snRNA-Seq data.** The relationship between number of cells in replicate
700 and median CV was tested in ROSMAP (A) and autism_PFC (B) dataset. Samples were colored
701 by RIN. Red dashed line denotes the CV threshold of 0.1. (C) & (D) illustrate the relationship
702 between RIN and median CV when replicate containing 200 cells in ROSMAP and autismPFC
703 data, respectively. Linear regression model was used. RIN, RNA integrity number.



704

705

706 **Figure 6 Relationship between expression accuracy and cell number.** **A.** Illustration of
707 expression accuracy assessment. **B.** The relationship between cell number and number of genes
708 with good accuracy is defined by Pearson correlation and linear regression model.



709

710 **Figure 7 Reproducibility of differential expression analysis in scRNA-Seq data. A.** True
 711 positive rate of DEGs in data with different numbers of cells. Datasets from different species are
 712 colored. **B.** True positive rate of DEGs with different effect sizes categorized by logFC of
 713 differential expression. **C.** The relationship between signal-to-noise ratio (SNR), and DEG
 714 reproducibility in mouse data. **D.** Model of DE reproducibility.

715 **Table 1 Single-cell/nuclei RNA sequencing datasets assessed in this study**

Data label	Species	PMID	Tissue	#Samples	#Cells	#Genes	#Cell types	Platform
ROSMAP	Human	3104269 7	Prefrontal cortex	24	75,060	17,926	8	10X
autism_PFC	Human	3109766 8	Prefrontal cortex	10	29,900	27,563	8	10X
autism_ACC	Human	3109766 8	Anterior cingulate	16	22,065	27,072	8	10X

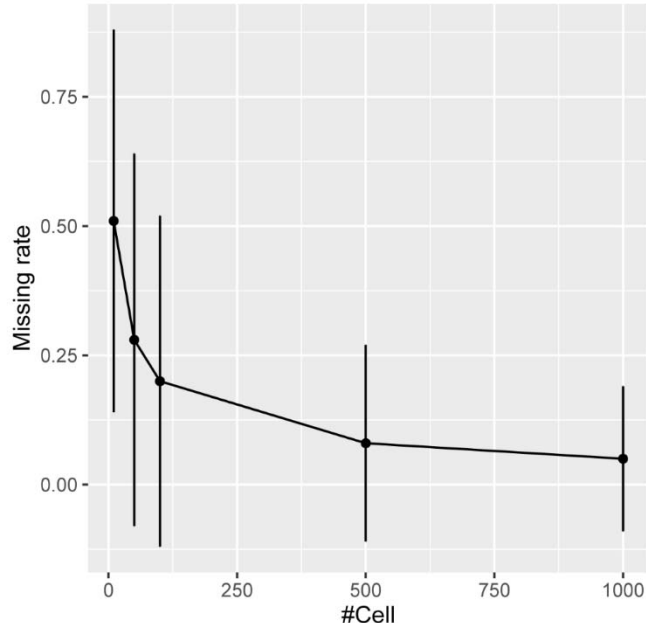
cortex								
MTG	Human	31435019	Medial temporal gyrus	8	15,583	43,474	7	Smart-Seq
M1_10X	Human	34616062	Primary motor cortex	2	76,533	27,933	8	10X
GSE97930_vc	Human	29227469	Visual cortex	3	19,368	21,273	8	Drop-seq
GSE97930_fro	Human	29227469	Frontal cortex	1	19,368	18,751	8	Drop-seq
GSE140231	Human	32826893	Cortex	5	10,581	24,702	6	10X
TREM	Human	31932797	Prefrontal cortex	11	36,671	36,601	6	10X
GSE174367	Human	34239132	Prefrontal cortex	8	21,996	25,392	6	10X
BICCN_adult	Human	37824663	Cortex	4	130,5075	19,762	30	10X
BICCN_HVS	Human	37824649	Cortex	78	353,194	18,797	24	10X
BICCN_trimester1	Human	37824650	Cortex	21	789,139	33,538	12	10X
BICCN_dev	Human	37824647	Cortex	106	709,372	19,005	9	10X
Tabula Sapiens	Human	35549404	Lung	3	33,222	23,739	3	10X
Tabula Sapiens	Human	35549404	Blood	6	37,892	21,147	1	10X
Tabula	Human	3554940	Lymph	3	47,891	22,271	1	10X

Sapiens		4	node						
Thrupp et al	Human	3299799 4	Microglia	3	14,823	21,015	1	10X	
Thrupp et al	Human	3299799 4	Microglia	3	3940	27,891	1	10X (whole cell)	
Hagai et al*	Mouse	3035622 0	Mononuc lear phagocyt es	6	17,776	15,319	1	Smart- seq2	
Hagai et al *	Rat	3035622 0	Mononuc lear phagocyt es	6	13,277	15,150	1	Smart- seq2	
Hagai et al *	Rabbit	3035622 0	Mononuc lear phagocyt es	6	17,097	9263	1	Smart- seq2	
Hagai et al *	Pig	3035622 0	Mononuc lear phagocyt es	6	12,753	8906	1	Smart- seq2	

716 *Note: *With sample-matched sorted-cell RNA-Seq data*

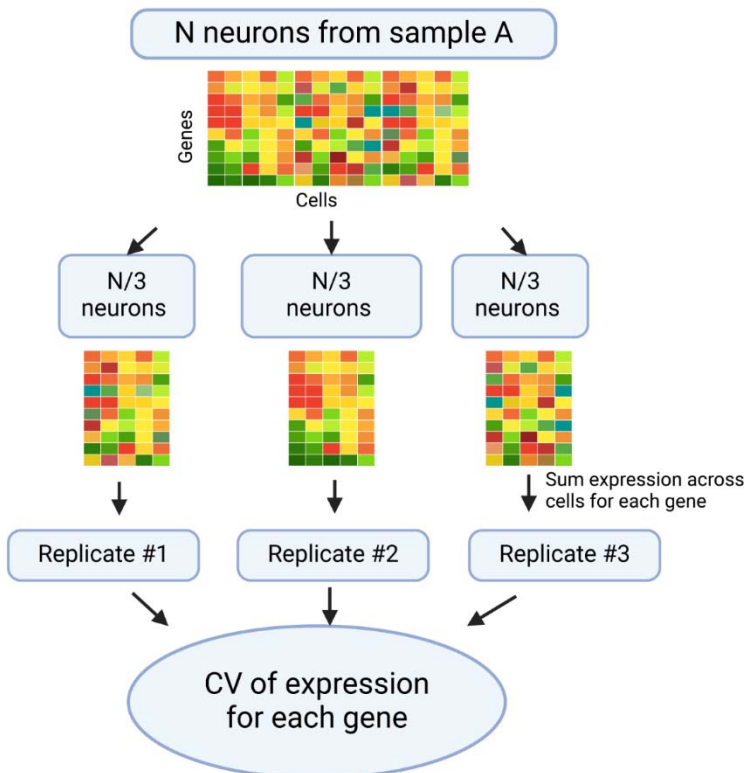
717

718 **Supplementary materials**



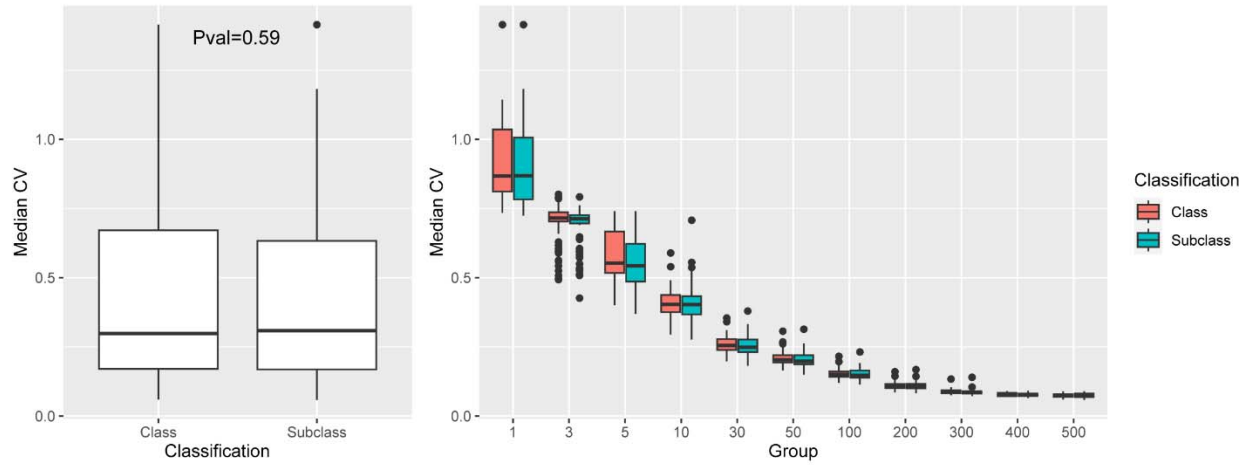
719

720 **Figure S1 Per gene missing rate in pseudo-bulk data with different number of cells.** Missing
721 rate was defined as proportion of zeros in all samples. Data from ROSMAP was used for the
722 demonstration.

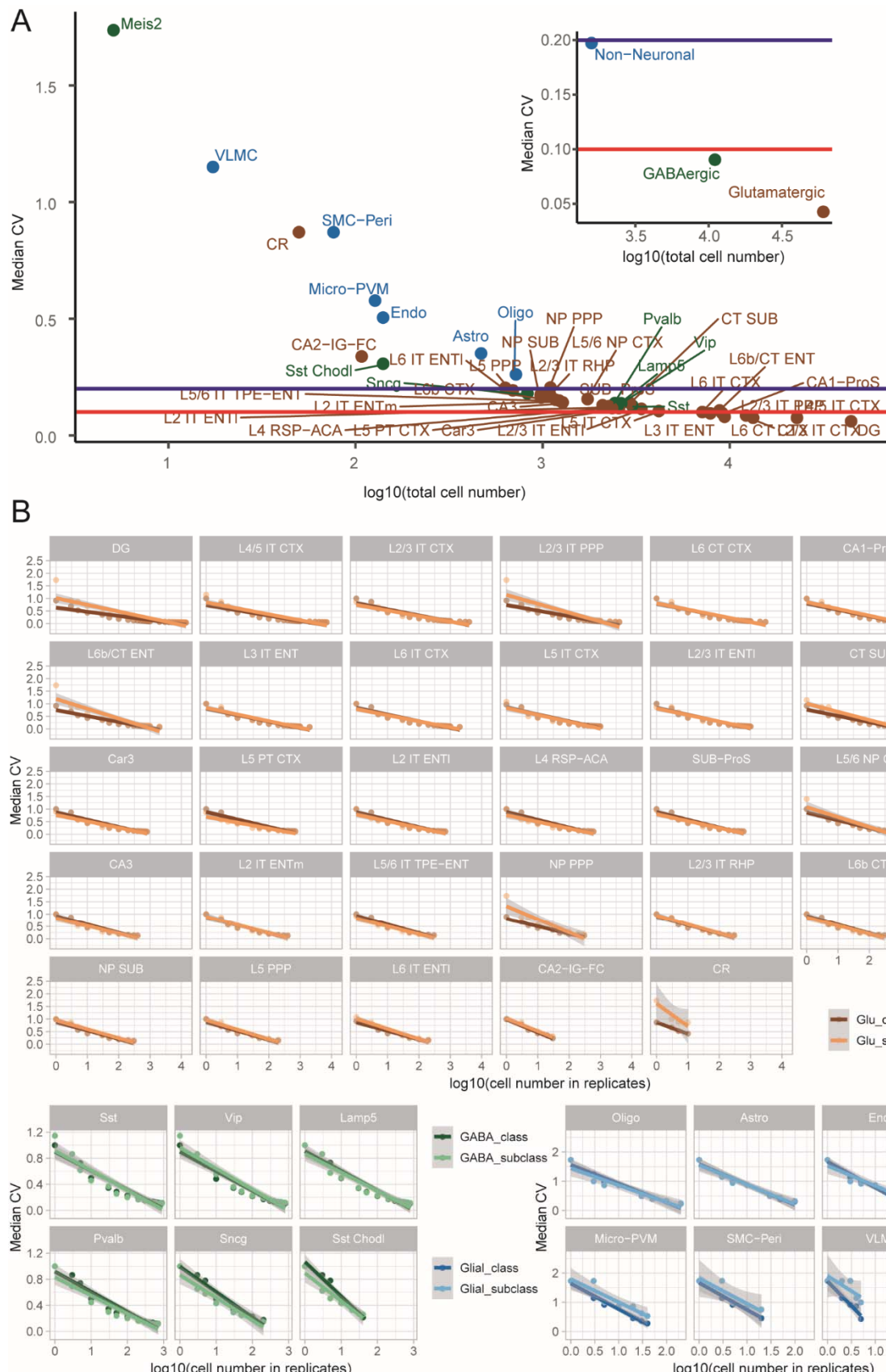


723

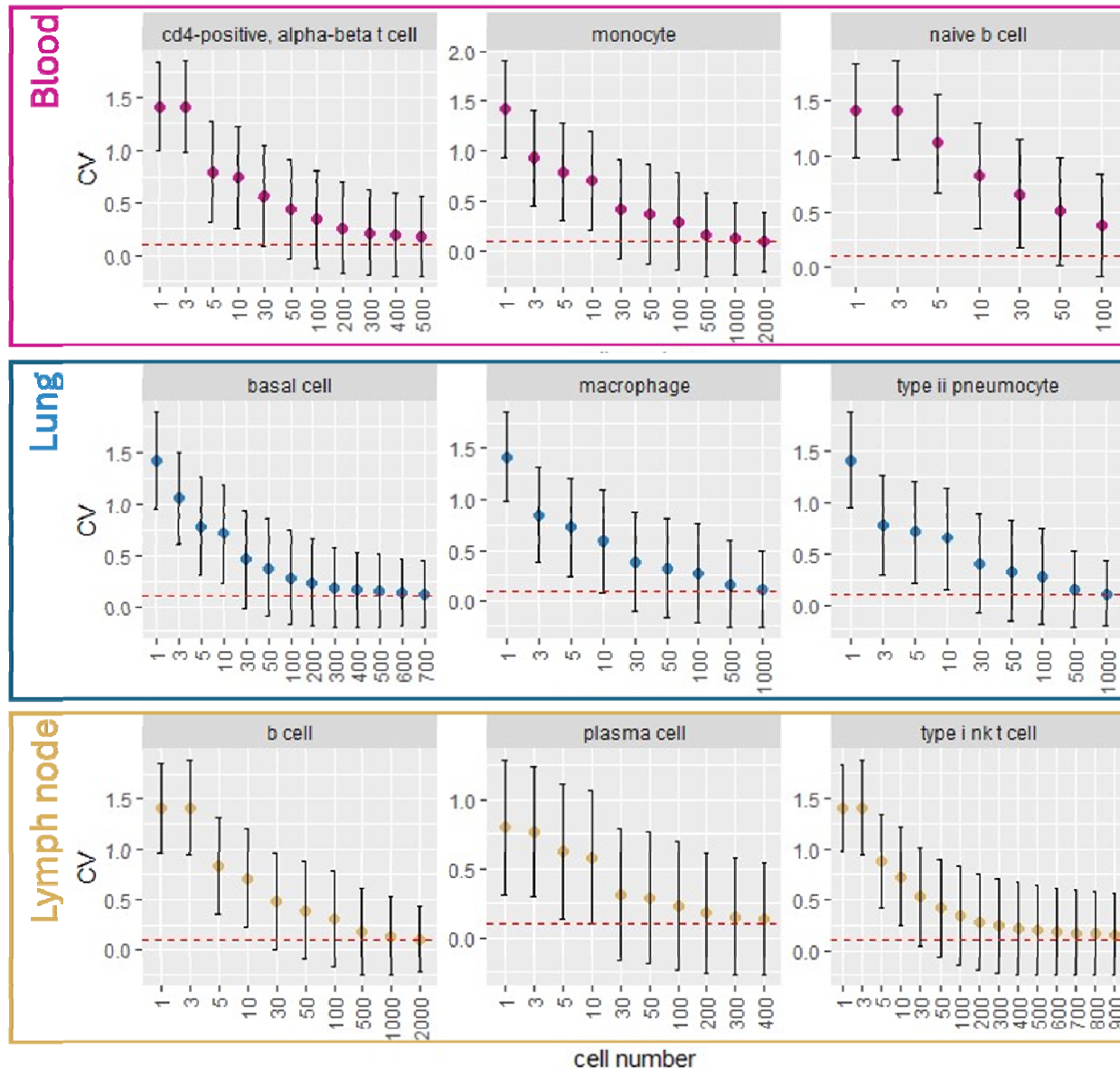
724 **Figure S2 Illustration of constructing technical replicates and calculating the CV of**
725 **expression across technical replicates. CV, coefficient of variation.**



726
727 **Figure S3 Expression variability at class and subclass level for excitatory neurons.** Data
728 from BICCN_HVS was used. P value was calculated with Student's T-Test.

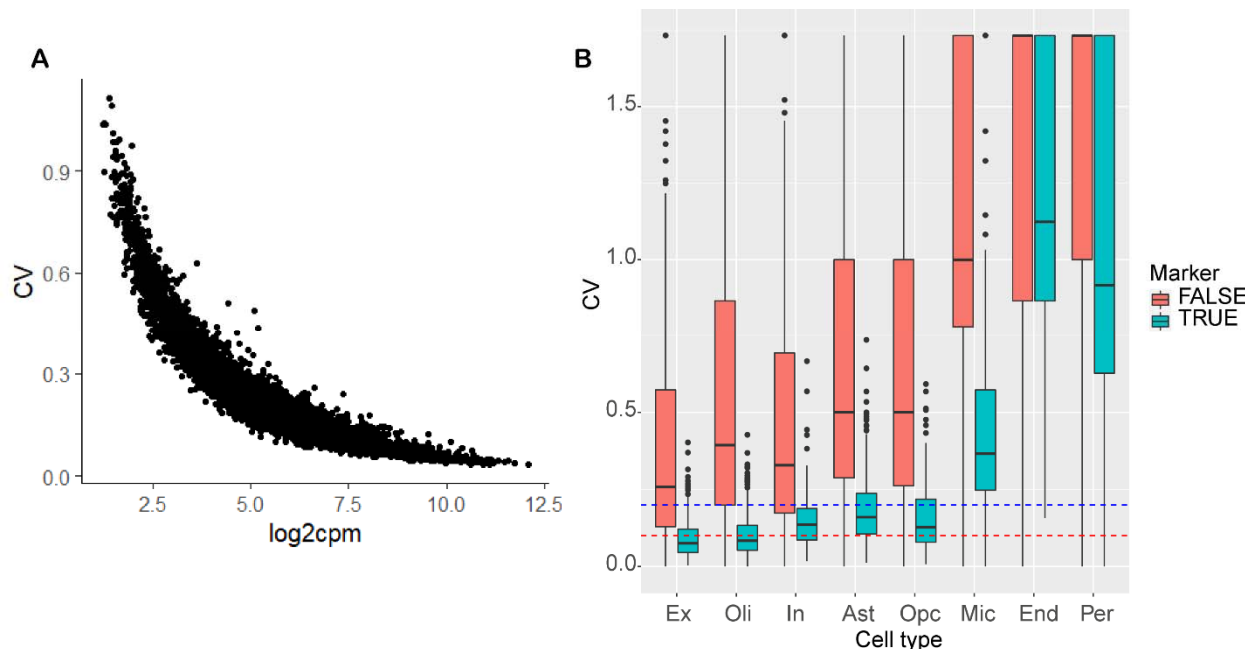


730 **Figure S4 Gene expression variability across technical replicates in mouse brain snRNA-
731 Seq data. A. Median CV across genes in replicates constructed at class and subclass level. B.
732 Linear regression model of cell numbers in replicates and median CV identified at class and
733 subclass level.**



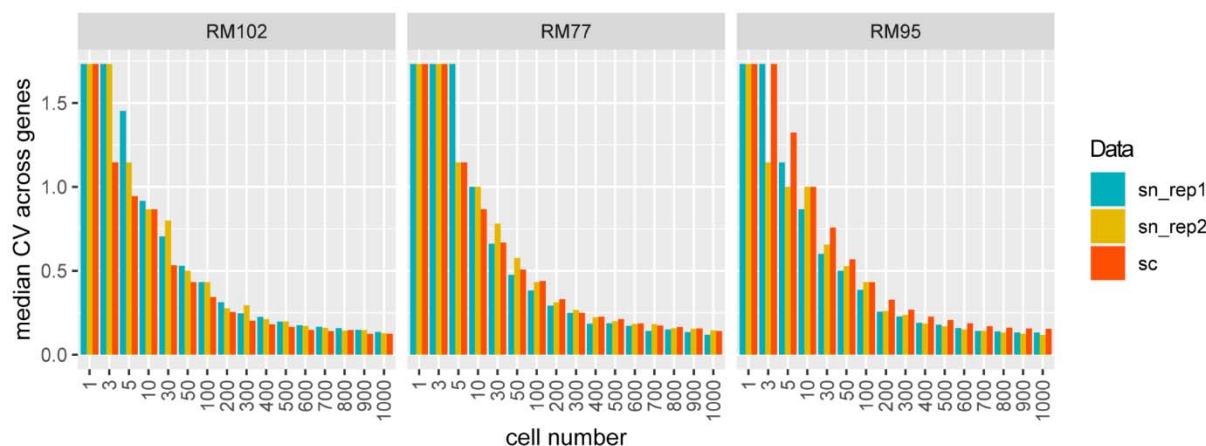
734

735 **Figure S5 Reduction of CV with the increased number of cells sequenced in three non-
736 brain tissues.** Data from Tabula Sapiens Consortium was used. Red line denotes CV of 0.1.



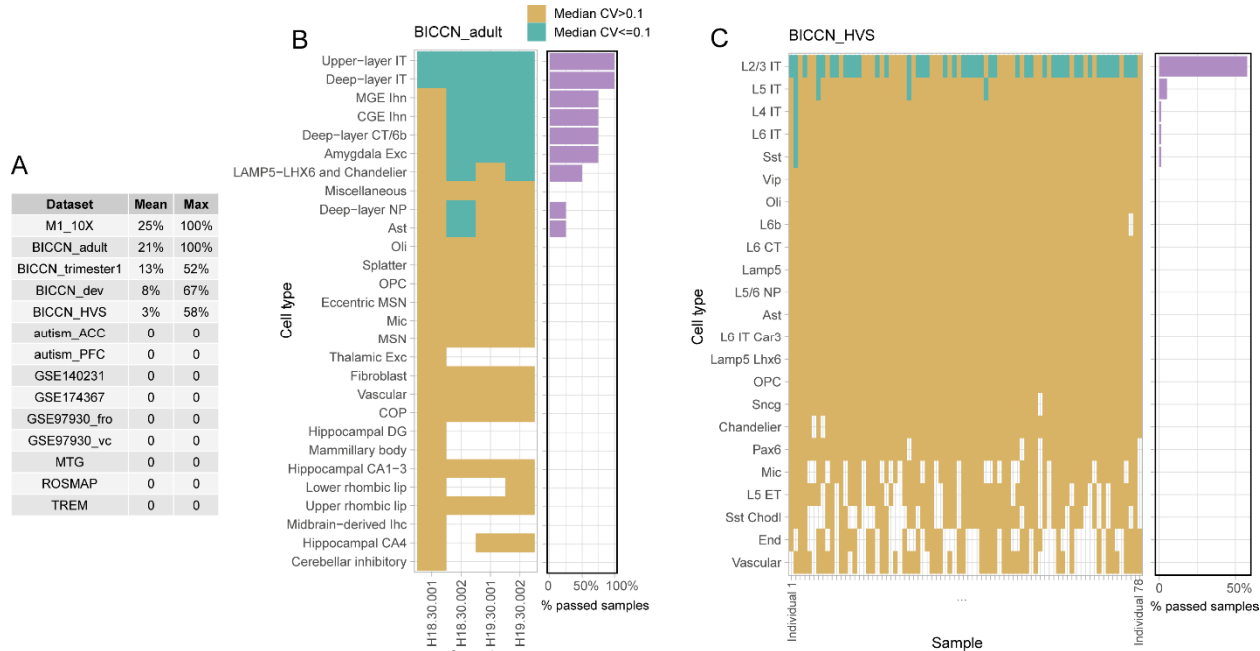
737

738 **Figure S6 Expression abundance and CV in ROSMAP data. A.** Relationship of expression
739 and CV in excitatory neuron from ROSMAP study. **B.** CV of marker genes. Blue and red line
740 denote CV of 0.2 and 0.1.



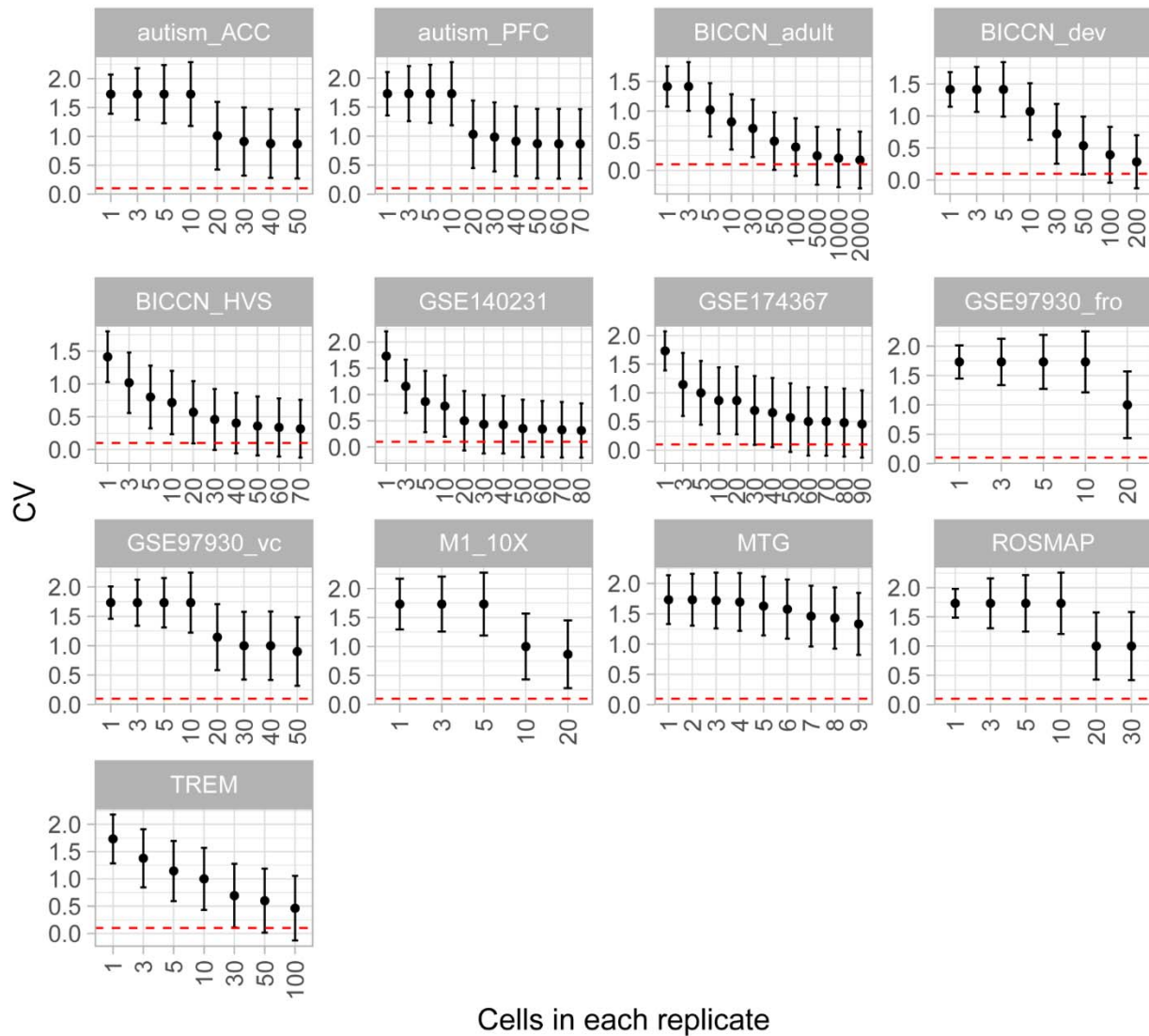
741

742 **Figure S7 Expression variability in scRNA-seq and snRNA-seq data.** Three human microglia
743 samples with both sc- and snRNA-Seq data are shown.



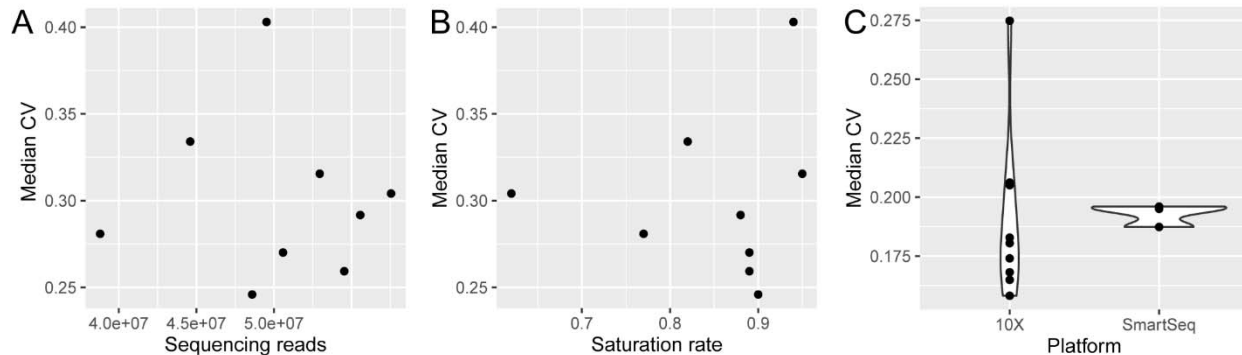
744

745 **Figure S8 Proportions of samples with acceptable expression variability.** A. The average and
 746 maximum percentages of samples that satisfy the precision criterion. Examples from
 747 BICCN_adult (B) and BICCN_HVS(C) datasets were used for illustration. Samples achieving
 748 the precision threshold, defined by a CV of 0.1 or lower, are indicated in green, signifying
 749 acceptable expression precision, while those failing to meet the threshold are marked in yellow,
 750 indicating low precision. Instances where a cell type is not represented in a sample are left blank.
 751 The accompanying bar plot provides a detailed breakdown of the exact proportion of samples
 752 that satisfy the precision criterion.



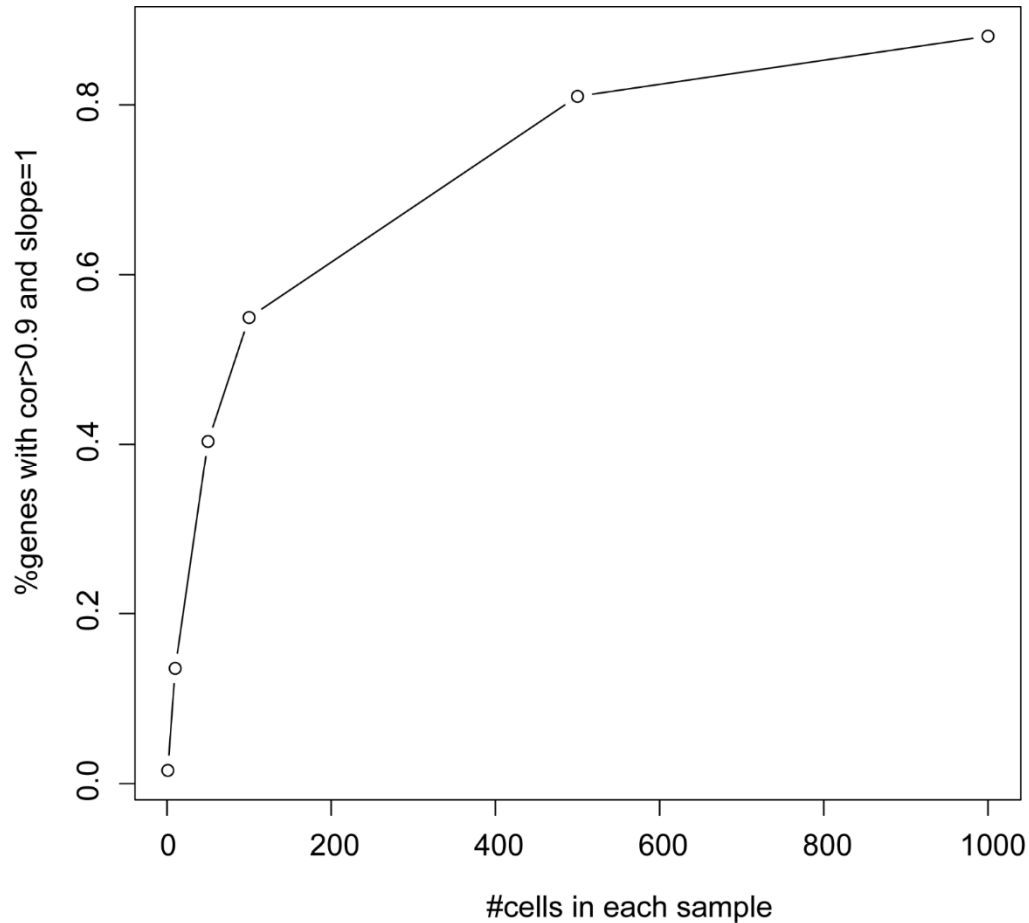
753

754 **Figure S9 Expression variability across replicates in human microglia.**



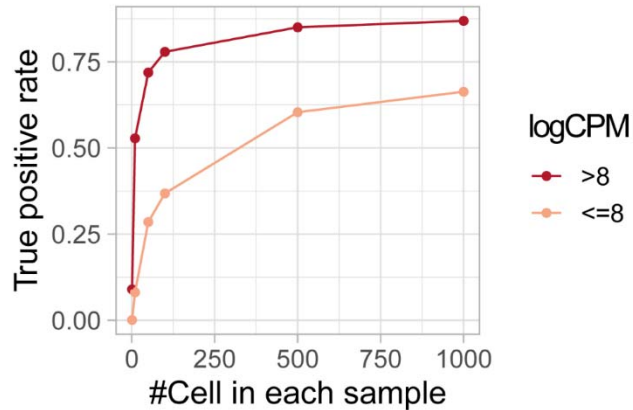
755

756 **Figure S10 Association between technical factors and gene expression variability across**
757 **technical replicates in snRNA-Seq data. A.** Median CV across detected genes in replicates
758 versus total sequencing depth. **B.** Median CV across detected genes in replicates versus total
759 sequencing saturation rate. **C.** Comparison of median CV across detected genes in replicates
760 between data sequenced by 10X Chromium and Smart-Seq platforms.



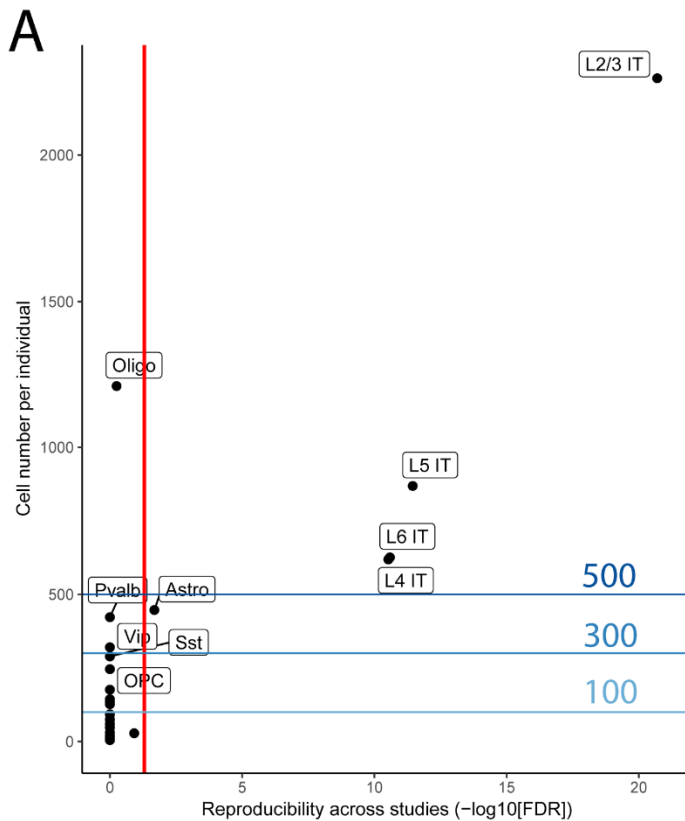
761

762 **Figure S11 Relationship between expression accuracy and the number of cells in simulated**
763 **data.** The X-axis represents the number of cells in each sample, and the Y-axis shows the
764 percentage of genes with good accuracy, as defined by Pearson correlation and a linear regression
765 model.



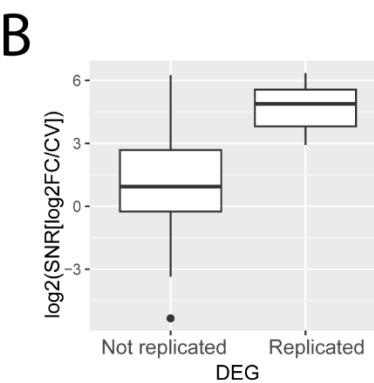
766

767 **Figure S12 True positive rate of DEGs with different expression levels categorized by log-**
768 **transformed counts per million (CPM).**



769

770 **Figure S13 Applying the 500-cell threshold and SNR to schizophrenia case-control scRNA-**
771 **seq data (Ruzicka et al).** A. Impact of cell number cutoff on the reproducibility of DEGs in two
772 schizophrenia cohorts. The plot illustrates the effect of different cell number cutoffs on the



773 reproducibility of DEGs identified in two independent schizophrenia cohorts (MCL and Mt
774 Sinai). **B.** The relationship between SNR and DEG reproducibility in astrocytes.

775 **Table S1 Expression accuracy statistics in datasets from four species**

776

777

778